Journal of Statistical Physics, Vol. 110, Nos. 1/2, January 2003 (© 2003)

Mean First-Passage Time in the Stochastic Theory of Biochemical Processes. Application to Actomyosin Molecular Motor

M. Kurzyński and P. Chełminiak[1]

Received July 26, 2001; accepted June 28, 2002

Many studies performed in recent years indicate a rich stochastic dynamics of transitions between a multitude of conformational substates in native proteins. A slow character of this dynamics is the reason why the steady-state kinetics of biochemical processes involving protein enzymes cannot be described in terms of conventional chemical kinetics, i.e., reaction rate constants. A more sophisticated language of mean first-passage times has to be used. A technique of summing up the stochastic dynamics diagrams is developed, enabling a calculation of the steady-state fluxes for systems of enzymatic reactions controlled and gated by the arbitrary type stochastic dynamics of the enzymatic complex. For a single enzymatic reaction, it is shown that the phenomenological steady-state kinetics of Michaelis–Menten type remains essentially unaltered but the interpretation of its parameters needs substantial change. A possibility of dynamical rather then structural inhibition of enzymatic activity is supposed. Two coupled enzymatic cycles are studied in the context of the biologically important process of free energy transduction. The theoretical tools introduced are applied to elucidate the mechanism of mechanochemical coupling in actomyosin molecular motor. Relations were found between basic parameters of the flux-force dependences: the force stalling the motor, the degree of coupling between the ATPase and the mechanical cycles as well as the asymptotic turnover number, and the mean first-passage times in a random movement between the particular conformational substates of the myosin head. These times are to be determined within a definite model of conformational transition dynamics. The theory proposed, not contradicting the presently available experimental data, is capable

[1] Institute of Physics, Adam Mickiewicz University, Umultowska 85, 61-614 Poznań, Poland; e-mail: kurzphys@main.amu.edu.pl

0022-4715/03/0100-0137/0 © 2003 Plenum Publishing Corporation

to explain the recently demonstrated multiple stepping produced by a single myosin head during just one ATPase cycle.

KEY WORDS: Protein dynamics; stochastic theory of reaction rates; first-passage time; enzymatic catalysis; free energy transduction; actomyosin molecular motor.

1. INTRODUCTION

Statistical theory of any physical process has to be based on simple but adequate models of phenomena underlying microscopic dynamics. Remarkable progress in studies of internal dynamics of biomolecules acomplished in recent years[1–5] has made it possible to formulate such models also for the basic biochemical processes. It is now clearly established that apart from the usual internal vibrations the native biomolecules, in particular protein enzymes, reveal also a rich stochastic dynamics of transitions between a multitude of conformational substates. Except some very fast processes of electron transfer, typical time scales of biochemical processes range from microseconds to seconds, hence the macromolecular normal vibrations are too fast to essentially influence these processes. Only the slower, stochastic dynamics of conformational transitions can affect the majority of biochemical processes. As a consequence, any adequate statistical theory of these processes has to be a development of the stochastic theory of reaction rates.[6–8]

The relaxation time spectrum characterizing the conformational transition dynamics of native proteins seems to be practically quasi-continuous, at least in the range from 10^{-11} to 10^{-7} s.[5] Two classes of mathematical models of the stochastic dynamics with such a property can be proposed. In the first class, of the *protein machine* type,[5,9] the dynamics of conformational transitions is represented by a quasi-continuous diffusion in a certain effective potential along one or a few "mechanical" coordinates, e.g., angles or distances describing mutual orientation of approximately rigid fragments of protein secondary structure (α-helices, β-plated sheets) or larger structural elements. The mechanical coordinate may be also identified with a "reaction coordinate," if this can be determined. The spectrum of reciprocal relaxation times for dynamics of the protein machine type is more or less homogeneous. Otherwise, in the second class of models of the *protein glass* type[5,10] the spectrum of reciprocal relaxation times is assumed to have a self-similarity symmetry. Time scaling, often observed in the case of protein involving reactions,[3–5] can originate either from a hierarchy of barrier heights in the conformational potential energy landscape[3,4] or from a hierarchy of bottlenecks (the entropy barrier heights) in the network joining conformations between which direct transitions take place. Such networks are represented by fractal lattices.[10,11]

The essential majority of reactions involving protein enzymes are *controlled* and, presumably, also *gated* by the intramolecular dynamics of conformational transitions.[5] To explain what do these two notions, important to the subject of the present paper, mean, we present in Fig. 1 an exemplifying realization of the microscopic (or rather mezoscopic) stochastic dynamics underlying a unimolecular reaction

$$M_1 \leftrightarrow M_2$$

between two chemical species M_1 and M_2 of the protein macromolecule or its complex with a low-molecular weight substrate. The chemical reaction is realized through the transitions between distinguished conformational substates in M_1, jointly forming what is called the transition state $M_1^{\ddagger}$, and distinguished conformational substates in M_2, jointly forming the transition state $M_2^{\ddagger}$. Two limiting cases can be formally distingushed. The one, where both transition states comprise all the conformational substates in M_1 and M_2, referred to as a reaction with *fluctuating barriers* (each conformational substate is related to a generally different free energy barrier for the reactive transition). And the opposite, of the transition states

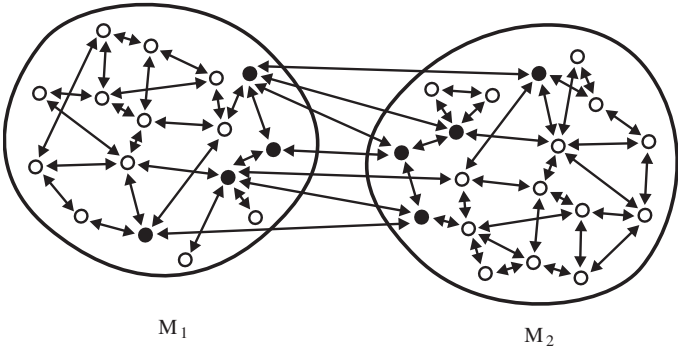

Fig. 1. Exemplifying realization of the model intramolecular dynamics underlying the unimolecular reaction $M_1 \leftrightarrow M_2$ discussed. Chemical states M_1 and M_2 of a macromolecule are composed of many conformational substates (white and black circles) and the intramolecular dynamics involves purely stochastic conformational transitions (the arrows). Actually, a much larger number of conformational substates are expected. The chemical reaction is realized through the transitions between distinguished conformational substates in M_1, jointly forming what is called the transition state $M_1^{\ddagger}$ (the black circles), and distinguished conformational substates in M_2, jointly forming the transition state $M_2^{\ddagger}$. If the transition states comprise all the conformational substates in M_1 and M_2 we refer to such a situation as a reaction with fluctuating barriers and if the transition states are reduced to single conformational substates we talk about the gated reaction.

reduced to single conformational substates, joitly forming a "gate;" we say then about a *gated reaction*. The two concepts have been introduced in the context of protein reactions in 1980 by Frauenfelder and coworkers.[12]

In formal terms, the model dynamics is described by a system of master equations[13]

$$\dot{p}_l(t) = \sum_{l'} [w_{ll'} p_{l'}(t) - w_{l'l} p_l(t)]. \tag{1.1}$$

The quantity $p_l(t)$ denotes the probability of the macromolecule being in a conformational substate l at time t and the coefficients $w_{ll'}$ are the transition probabilities per unit time satisfying the detailed balance condition. The dot means a derivation with respect to time. The mole fractions

$$P_i(t) \equiv \sum_{l \in \mathrm{M}_i} p_l(t), \tag{1.2}$$

$i = 1, 2$ ($P_1(t) + P_2(t) = 1$), of protein molecules being at time t in the chemical state M_1 or M_2, respectively, proportional to the molar concentrations $[\mathrm{M}_1]$ or $[\mathrm{M}_2]$, satisfy the equation:

$$\dot{P}_1(t) = -\dot{P}_2(t) = -\sum_{l \in \mathrm{M}_1^{\ddagger}} \sum_{l' \in \mathrm{M}_2^{\ddagger}} [w_{l'l} p_l(t) - w_{ll'} p_{l'}(t)]. \tag{1.3}$$

In general the solution to it is non-exponential and depends on the initial values of all the probabilities p_l. However, if the reaction is an *activated process*, i.e., if transitions between the states M_1 and M_2 are rare when compared to the time of conformational relaxation, than, after the initial period equal to that time, Eq. (1.3) takes a form of the usual kinetic equation

$$\dot{P}_1(t) = -\dot{P}_2(t) = -k_+ P_1(t) + k_- P_2(t) \tag{1.4}$$

of the exponential solution.

The reciprocal forward reaction rate constant k_+^{-1} and the reciprocal backward reaction rate constant k_-^{-1} can be decomposed into three time components:[6–8]

$$k_+^{-1} = (k_+^{\mathrm{eq}})^{-1} + \tau_1 + K^{-1}\tau_2, \qquad k_-^{-1} = (k_-^{\mathrm{eq}})^{-1} + \tau_2 + K\tau_1. \tag{1.5}$$

Here K is the ratio

$$K \equiv k_+^{\mathrm{eq}} / k_-^{\mathrm{eq}}, \tag{1.6}$$

thus, due to the form of Eqs. (1.5), also the ratio

$$K = k_+ / k_-, \tag{1.7}$$

i.e., the chemical equilibrium constant. The first components in Eqs. (1.5) determine the time needed for reaction to proceed in a given direction under the assumption (made in the transition state theory[6,7]) that the corresponding transition state $M_i^{\ddagger}$ is in a local equilibrium within itself and with respect to the remaining substates in M_i. As a result of the proceeding reaction this equilibrium is, however, disturbed. These are the remining components in Eqs. (1.5) that determine the time needed for restoring this equilibrium, both from the side of M_1 and of M_2.

If all the three components in Eqs. (1.5) are comparable (as in the case of reactions of small molecules in the gas phase), the forward and backward reaction rate constants are well described by the transition state theory counterparts k_+^{eq} and k_-^{eq}, possibly with certain transmission coefficients smaller than unity. The initial stage of the reaction is then practically absent. If, on the contrary, the second and the third components prevail, the reaction is referred to as *controlled* by intramolecular dynamics and the transition state theory fails. In the latter case, the initial stage of the reaction can appear even to dominate.

That biochemical reactions are controlled by the intramolecular dynamics follows from the observation of some non-exponential initial stages.[3–5,12,14] The non-exponential initial stage is clearly seen in computer simulations of the time course of reaction gated and controlled by a model dynamics of random walk type.[11]

Direct observation of the initial stages of reactions in experiments and simulations was possible due to a special preparation of the initial conformational substates of the protein confined to the reaction transition state. Usually, the initial distribution of conformational substates is not much different from the local equilibrium and no initial condition-dependent stages are observed in the time course of biochemical reactions proceeding in standard conditions. But the specially prepared initial substates of protein macromolecules occur also in standard conditions, if several coupled reactions gated by conformational transition dynamics proceed in steady state. Because of the slow character of the intramolecular dynamics, the succeeding reactions proceed before the local equilibria in the preceding chemical species have been reached. As a consequence, the steady-state kinetics, like the initial stage kinetics, cannot be described in terms of the usual rate constants. This possibility was suggested already more then a quarter of a century ago by Blumenfeld.[15] More adequate physical quantities that should be used are the mean first-passage times.[5] The goal of

the present paper is to prove this formally for the protein involving reactions controlled and gated by an arbitrary stochastic dynamics of conformational transitions. Only models that assume gating in addition to the control by the intramolecular dynamics, when applied in description of the complete enzymatic cycles proceeding under the steady-state conditions, lead to the reconstruction of the commonly observed Michaelis–Menten kinetics.[16] This was shown specifically for the particular protein-machine model of intramolecular dynamics[9] and will be proven quite generally here.

The paper is organized as follows. After this short Introduction to the main concepts of the stochastic theory of reaction rates in application to proteins, a general technique of the mean first-passage time calculation is developed in Section 2 and a few theorems concerning the gated reactions are proven in Section 3. A detailed analysis of the steady-state kinetics of a single enzymatic cycle is presented in Section 4 whereas in Section 5 two coupled enzymatic cycles are studied in the context of the biologically important processes of free energy transduction. To show the usefulness of the theoretical tools introduced we apply them in Section 6 for elucidation of the mechanism of mechanochemical coupling in actomyosin molecular motor. Section 7 makes a summary. Some preliminary results have been already published elsewhere.[14, 17]

2. CALCULATION OF MEAN FIRST-PASSAGE TIMES

Let us consider a set of states M of a physical system with a certain stochastic dynamics determined by a set of master equations (1.1) with the transition probabilities per unit time, $w_{ll'}$, satisfying the detailed balance condition. The set M can be considered as a graph (diagram, lattice): the states of the system are represented by the vertices (points, sites) and the direct transitions, determined by the non-zero w's, by the edges (lines, the nearest neighbours).[18] By definition,[13] to find the mean first-passage time from some initial to some final state of the diagram M, one has to put a statistical ensemble of the systems at the initial state and observe its stochastic evolution. Each system reaches the final state after a certain time. The average of these times is the mean first-passage time from the initial to final state. But one can observe also some equivalent infinite process for a single system, assuming that each time a given system reaches the final state the same system appears anew at the initial state. After a time long enough this will be the stationary flux in such a diagram that determines the mean first-passage time looked for.

More precisely, after Hill,[19] the mean first passage time $\tau_{\mathrm{M}}(l_0 \to l)$ from the state l_0 to l in the diagram M with absorption at the final state l

can be found as the reciprocal of a steady-state one-way cycle flux or a sum of such fluxes J in a modified diagram $\mathrm{M}_{l_0 \to l}$ in which the absorption transition or transitions are redirected to the starting state l_0 with a simultaneous elimination of the absorption state from the original diagram M. An illustrative example of such a modification is shown in Figs. 2(a) and (b). In formal terms

$$\tau_{\mathrm{M}}(l_0 \to l) = J^{-1} = \left(\sum_{l'} w_{ll'} p_{l'} \right)^{-1}, \tag{2.1}$$

where the probabilities $p_{l'}$ are solutions of a set of the master equations (1.1) for the modified diagram $\mathrm{M}_{l_0 \to l}$ under the steady-state boundary conditions, with some detailed balance conditions broken. A useful method for the calculation of such steady-state probabilities and fluxes is offerd by the technique of summing up the directional diagrams described in an algorithmic way in the already mentioned book by Hill.[19]

The Hill's algorithm of finding the steady-state (or the equilibrium, in the case when the detailed balance condition is satisfied for each transition) probability p_l for an arbitrary diagram S comprises the following steps:

(i) Construction of the complete set of *partial diagrams* for S, each of which contains the maximum possible number of lines that can be included in the diagram without forming any cycle (closed path).

(ii) Construction of *directional diagrams*, for each state l and each partial diagram, if possible, in which all connected paths are directed *toward* and *end* at the state l. The directional diagram is uniquely attributed with a number equal to the product of transition probabilities corresponding to all directed lines involved.

(iii) Calculation of the sum of all directional diagrams of each state l in S, further denoted as $D_l(\mathrm{S})$, and than the sum of all directional diagrams in S

$$D(\mathrm{S}) \equiv \sum_{l \in \mathrm{S}} D_l(\mathrm{S}). \tag{2.2}$$

The steady-state (or equilibrium) occupation probability of the state l is determined by the ratio

$$p_l = \frac{D_l(\mathrm{S})}{D(\mathrm{S})}. \tag{2.3}$$

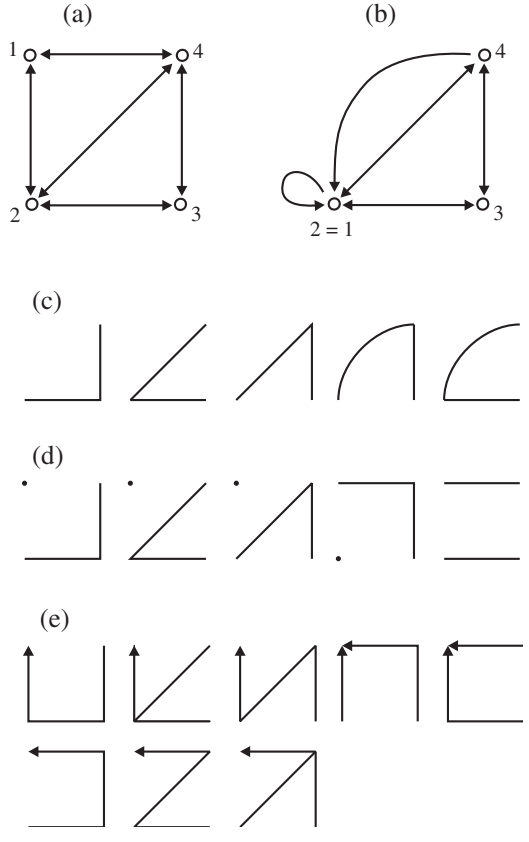

Fig. 2. (a) An example of the diagram M determing certain stochastic dynamics. (b) The modification $\mathrm{M}_{2\to 1}$ of the adjoining diagram, used in the calculation of the mean first-passage time $\tau_{\mathrm{M}}(2\to 1)$. (c) A complete set of partial diagrams for the modified diagram $\mathrm{M}_{2\to 1}$. (d) A complete set of partial diagrams for three possible dissections of the original diagram M into a subdiagram containing site 1 and a subdiagram containing site 2. It is seen that, if isolated sites counted as unity are disregarded, the set (d) of diagrams is identical to the set (c). (e) On multiplying diagrams in the set (d) by appropriate transition probabilities to the final site 1 one gets a set of diagrams which is identical to the complete set of all directional diagrams for site 1 in the original diagram M.

On applying this algorithm to the the probabilities $p_{l'}$ in Eq. (2.1) we get

$$\tau_{\mathrm{M}}(l_0 \to l) = \frac{\sum_{l'} D_{l'}(\mathbf{M}_{l_0 \to l})}{\sum_{l'} w_{ll'} D_{l'}(\mathbf{M}_{l_0 \to l})}. \tag{2.4}$$

To proceed further on it is essential to note that the complete set of partial diagrams for the modified diagram $M_{l_0 \to l}$ is identical to the complete set of partial diagrams for all possible dissections of M into sums of the form $M_{l_0} \cup M_l$, the subdiagram M_{l_0} containing site l_0 and the subdiagram M_l containing site l (cf. example in Figs. 2(c) and (d)). As a consequence the numerator of Eq. (2.4) can be rewritten as a quantity

$$D_{l,l_0}(M) \equiv \sum_{M_{l_0} \cup M_l} D_l(M_l)\, D(M_{l_0}), \tag{2.5}$$

with the summation running over all possible dissections $M_{l_0} \cup M_l$ of M, and the denominator of Eq. (2.4) equals simply the sum of all directional diagrams of the final state l in M (cf. Fig. 2(e)), thus

$$\tau_M(l_0 \to l) = \frac{D_{l,l_0}(M)}{D_l(M)}. \tag{2.6}$$

In the example considered in Fig. 2 the numerator consists of 12 different terms of the form of products of two possible transition probabilities allowed in five diagrams presented in Fig. 2(d) (the points count as unity), whereas the denominator consists of 8 terms of the form of products of three transition probabilities, presented directly in Fig. 2(e).

It is worth noting that the equilibrium (and only equilibrium!) occupation probabilities p_l can also be calculated for any subdiagram M′ of M comprising the state l. One only has to use the notion of the conditional probability and replace Eq. (2.3) with a more general equation

$$p_l = \frac{D_l(M')}{D(M')} P^{eq}(M'), \tag{2.7}$$

whith the quantity

$$P^{eq}(M') \equiv \sum_{l \in M'} p_l \tag{2.8}$$

having a meaning of the equilibrium occupation probability of the subset of states M′. On comparing Eqs. (2.7) and (2.3) we obtain a relation

$$D_l(M)\, D(M') = D_l(M')\, D(M)\, P^{eq}(M') \tag{2.9}$$

fulfilled for arbitrary l in M′. The reasoning does not apply to the steady-state occupation probabilities, with the detailed balance conditions broken, as a cut out of the subdiagram may perturb some probability fluxes.

With the help of Eq. (2.9) the sum of the forward and backward mean first-passage times can be rewritten in a symmetrical form:

$$\tau_{\mathrm{M}}(l_0 \leftrightarrow l) \equiv \tau_{\mathrm{M}}(l_0 \to l) + \tau_{\mathrm{M}}(l \to l_0) = \frac{D(\mathrm{M})\, S_{l_0,\,l}(\mathrm{M})}{D_{l_0}(\mathrm{M})\, D_l(\mathrm{M})}, \tag{2.10}$$

where

$$S_{l_0,\,l}(\mathrm{M}) = S_{l,\,l_0}(\mathrm{M}) \equiv \sum_{\mathrm{M}_{l_0} \cup \mathrm{M}_l} D_{l_0}(\mathrm{M}_{l_0})\, D_l(\mathrm{M}_l) \tag{2.11}$$

with the summation running over all possible dissections $\mathrm{M}_{l_0} \cup \mathrm{M}_l$ of M, the subdiagram M_{l_0} containing l_0 but not l and the subdiagram M_l containing l but not l_0.

For an arbitrary state $l' \in \mathrm{M}$, different both from l_0 and l, the class of all possible dissections $\mathrm{M}_{l_0} \cup \mathrm{M}_l$ of the diagram M subdivides itself into two subclasses of dissections of the form $\mathrm{M}_{l_0 l'} \cup \mathrm{M}_l$, the subdiagram $\mathrm{M}_{l_0 l'}$ containing l_0 and l' but not l and the subdiagram M_l containing l but not l_0 and l', and of the form $\mathrm{M}_{l_0} \cup \mathrm{M}_{ll'}$, the subdiagram M_{l_0} containing l_0 but not l and l' and the subdiagram $\mathrm{M}_{ll'}$ containing l and l' but not l_0.[2] With this subdivision Eq. (2.6) can be written as

$$\tau_{\mathrm{M}}(l_0 \to l) = \sum_{\mathrm{M}_{l_0 l'} \cup \mathrm{M}_l} \frac{D_l(\mathrm{M}_l)\, D(\mathrm{M}_{l_0 l'})}{D_l(\mathrm{M})} + \sum_{\mathrm{M}_{l_0} \cup \mathrm{M}_{ll'}} \frac{D_l(\mathrm{M}_{ll'})\, D(\mathrm{M}_{l_0})}{D_l(\mathrm{M})}. \tag{2.12}$$

The first sum determines the mean first-passage time from l_0 to l provided l' has been reached before l and the second sum determines the mean first-passage time from l_0 to l provided l' has not been reached before l. In other words, the first sum is the mean first-passage time from l_0 *or* l' to l and the second sum, the mean first-passage time from l_0 to l *or* l'. This justifies the notations

$$\sum_{\mathrm{M}_{l_0 l'} \cup \mathrm{M}_l} \frac{D_l(\mathrm{M}_l)\, D(\mathrm{M}_{l_0 l'})}{D_l(\mathrm{M})} \equiv \tau_{\mathrm{M}}(\{l_0, l'\} \to l) \tag{2.13}$$

and

$$\sum_{\mathrm{M}_{l_0} \cup \mathrm{M}_{ll'}} \frac{D_l(\mathrm{M}_{ll'})\, D(\mathrm{M}_{l_0})}{D_l(\mathrm{M})} = \sum_{\mathrm{M}_{l_0} \cup \mathrm{M}_{ll'}} \frac{D_{l'}(\mathrm{M}_{ll'})\, D(\mathrm{M}_{l_0})}{D_{l'}(\mathrm{M})} \equiv \tau_{\mathrm{M}}(l_0 \to \{l, l'\}) \tag{2.14}$$

[2] One subclass can be empty as for, e.g., one-dimensional diagrams.

(the equality results from the relation (2.9)), with the help of which Eq. (2.12) can be rewritten as

$$\tau_{\mathrm{M}}(l_0 \to l) = \tau_{\mathrm{M}}(\{l_0, l'\} \to l) + \tau_{\mathrm{M}}(l_0 \to \{l, l'\}). \tag{2.15}$$

Let us consider the sum of the forward and backward mean first-passage times of the form

$$\tau_{\mathrm{M}}(l' \leftrightarrow \{l, l''\}) \equiv \tau_{\mathrm{M}}(l' \to \{l, l''\}) + \tau_{\mathrm{M}}(\{l, l''\} \to l'). \tag{2.16}$$

An application of the relation (2.9) results in a formula

$$\tau_{\mathrm{M}}(l' \leftrightarrow \{l, l''\}) = \frac{D(\mathrm{M})\, S_{l''(l),\, l'}(\mathrm{M})}{D_{l''}(\mathrm{M})\, D_{l'}(\mathrm{M})}, \tag{2.17}$$

where

$$S_{l''(l),\, l'}(\mathrm{M}) \equiv \sum_{\mathbf{M}_{ll''} \cup \mathbf{M}_{l'}} D_{l''}(\mathbf{M}_{ll''})\, D_{l'}(\mathbf{M}_{l'}). \tag{2.18}$$

Let us note yet a relation

$$\tau_{\mathrm{M}}(l' \leftrightarrow \{l, l''\}) + \tau_{\mathrm{M}}(\{l, l'\} \leftrightarrow l'') = \tau_{\mathrm{M}}(l' \leftrightarrow l''), \tag{2.19}$$

which follows directly from Eq. (2.15). The quantity (2.16), the formula (2.17) and the relation (2.19) will be very useful in Section 5, where we shall be considering two coupled enzymatic reactions.

3. APPLICATION TO GATED REACTIONS

Having derived two formulae (2.6) and (2.10) for the calculation of mean first-passage times we now prove three general theorems of increasing complexity, useful in the theory of reactions controlled and gated by the intramolecular stochastic dynamics. The notation used is explained in Figs. 3(a)–(c), where diagrams of intramolecular dynamics between an arbitrary number of conformational substates within a given chemical molecular state are represented by shaded boxes. Figures 3(a) and 3(b) present irreversible gated reaction—the product state is replaced by the completely absorbing *limbo state*[13] denoted by the asterisk. It should be stressed that the zero transition probability in the backward direction does not mean here that the detailed balance is broken but that the equilibrium occupation probability of the initial chemical state P^{eq} is zero.

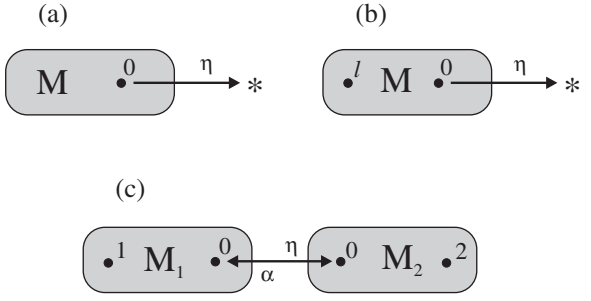

Fig. 3. Illustrations to Theorem 1 (a), Theorem 2 (b), and Theorem 3 (c). Shaded boxes represent diagrams of an arbitrary number of sites and the direct transitions between them. The asterisk denotes the completely absorbing limbo state.

Theorem 1. The mean first-passage time between the transition state 0 of a reaction and the limbo state $*$ equals the reciprocal of the transition state theory rate constant:

$$\tau(0 \to *) = (k_+^{\mathrm{eq}})^{-1}, \tag{3.1}$$

where

$$k_+^{\mathrm{eq}} = (p_0^{\mathrm{eq}} / P^{\mathrm{eq}})\, \eta, \tag{3.2}$$

the ratio p_0^{eq} over P^{eq} being the local equilibrium probability of the transition state occupation (it should be interpreted in terms of the conditional probability, Eq. (2.8), otherwise it equals zero over zero) and η, the transition probability per unit time through the gate from the transition state 0 to the limbo state (Fig. 3(a)).

Proof. From Eqs. (2.6), (2.18) and (2.7) we have

$$\tau(0 \to *) = \frac{D_{*,0}(\mathrm{M}^*)}{D_*(\mathrm{M}^*)} = \frac{D(\mathrm{M})}{\eta D_0(\mathrm{M})} = \frac{P(\mathrm{M})}{\eta p_0},$$

where M^* denotes the diagram M describing an internal dynamics within a species M, extended by the transition η to the limbo state $*$ (Fig. 3(a)). Because the detailed balance condition in M is not broken, any steady-state probability equals the equilibrium one.

Theorem 2. For an arbitrary state l in M

$$\tau(l \to *) = \tau_{\mathrm{M}}(l \to 0) + (\kappa^{\mathrm{eq}})^{-1} \tag{3.3}$$

(Fig. 3(b)).

Proof. There are two kinds of dissections possible of the diagram M* into the subdiagrams containg l and $*$: those leaving the transition η and the one passing through this transition, thus

$$\tau(l \to *) = \frac{D_{*,l}(\mathrm{M}^*)}{D_*(\mathrm{M}^*)} = \frac{\eta D_{0,l}(\mathrm{M}) + D(\mathrm{M})}{\eta D_0(\mathrm{M})}$$
$$= \frac{D_{0,l}(\mathrm{M})}{D_0(\mathrm{M})} + \frac{D(\mathrm{M})}{\eta D_0(\mathrm{M})} = \tau_{\mathrm{M}}(l \to 0) + (\kappa^{\mathrm{eq}})^{-1}.$$

Theorem 3. Let the two diagrams M_1 and M_2 (representing the reagent and the product chemical state of a molecule) be connected by a reversible transition between the gates denoted as 0, of the probabilities per unit time η and α in the forward and backward direction, respectively (Fig. 3(c)). Then, for an arbitrary state 1 in M_1 and an arbitrary state 2 in M_2

$$\tau(1 \to 2) = (k_+^{\mathrm{eq}})^{-1} + \tau_{\mathrm{M}_1}(1 \to 0) + \tau_{\mathrm{M}_2}(0 \to 2) + K^{-1}\tau_{\mathrm{M}_2}(0 \leftrightarrow 2), \qquad (3.4)$$

where $\tau_{\mathrm{M}_i}(i = 1, 2)$ denote the mean first-passage times confined to the corresponding subdiagrams. The quantity

$$K = \frac{k_+^{\mathrm{eq}}}{k_-^{\mathrm{eq}}} \qquad (3.5)$$

has a meaning of the reaction equilibrium constant,

$$k_+^{\mathrm{eq}} = \eta \frac{D_0(\mathrm{M}_1)}{D(\mathrm{M}_1)}, \qquad k_-^{\mathrm{eq}} = \alpha \frac{D_0(\mathrm{M}_2)}{D(\mathrm{M}_2)} \qquad (3.6)$$

corresponding, respectively, to the forward and backward transition state theory rate constants (cf. Eq. (2.7)).

Proof. Let M denote a sum of the diagrams M_1 and M_2 extended by the transition between the gates. There are three kinds of dissections possible of the diagram M into the subdiagrams containing 1 and 2: one passing through the very transition between the gates, those leaving the forward transition η and those leaving the backward transition α. Accordingly,

$$\tau(1 \to 2) = \frac{D_{2,1}(\mathrm{M})}{D_2(\mathrm{M})}$$
$$= \frac{D_2(\mathrm{M}_2)\, D(\mathrm{M}_1)}{D_2(\mathrm{M}_2)\, \eta D_0(\mathrm{M}_1)}$$

$$+\eta\,\frac{D_2(\mathrm{M}_2)\,D_{0,1}(\mathrm{M}_1)+D_{2,0}(\mathrm{M}_2)\,D_0(\mathrm{M}_1)}{D_2(\mathrm{M}_2)\,\eta D_0(\mathrm{M}_1)}$$

$$+\alpha\,\frac{D(\mathrm{M}_1)\,S_{2,0}(\mathrm{M}_2)}{D_2(\mathrm{M}_2)\,\eta D_0(\mathrm{M}_1)}.$$

On using the definitions (3.6) and Eq. (2.10) one gets the thesis (3.4).

For the state 2 being a typical (highly occupied at the equilibrium) state, the mean first passage time $\tau_{\mathrm{M}_2}(0\to 2)$ is much shorter than $\tau_{\mathrm{M}_2}(2\to 0)$ and can be neglected. Then Eq. (3.4) reconstructs the general expression (1.5) for the complete forward rate constant:

$$k_+^{-1}=(k_+^{\mathrm{eq}})^{-1}+\tau_{\mathrm{M}_1}(1\to 0)+K^{-1}\tau_{\mathrm{M}_2}(2\to 0), \tag{3.7}$$

and a similar for the backward one.

4. SINGLE ENZYMATIC REACTION

As the first application of the enginery developed in two previous sections let us consider the simplest, two step, generally reversible enzymatic reaction[16]

$$\mathrm{E}+\mathrm{R}\leftrightarrow\mathrm{M}\leftrightarrow\mathrm{E}+\mathrm{P}$$

(R and P stand for the reactant and the product, respectively, E stands for the free enzyme and M for the Michaelis enzyme-substrate complex). In the conventional approach all the microscopic substates of the enzymatic protein are assumed to reach a local equilibrium and in the steady state, for the molar concentrations of reactant [R] and product [P] kept constant, only the steady-state concentrations of the macroscopic species [E] and [M] have to be determined. For this purpose the knowledge of the values of the conventional kinetics rate constants $k'_\pm$ and $k''_\pm$ (Fig. 4(a)) is sufficient. However, if both component reactions are controlled by the intramolecular dynamics of conformational transitions, the steady-state occupation distribution is reached among the conformational substates instead of the local equilibrium one. Consequently, to describe the actual kinetic mechanism of enzymatic reaction one has to treat the conformational transitions on an equal footing with the chemical (here the binding-rebinding) transformations.[20] In Fig. 4(b) the multitudes of conformational transitions within E and M are represented, as in Fig. 3, by shaded boxes and both the component reactions are assumed to proceed through gates consisting of single (possibly effective) explicitly labelled conformational substates.

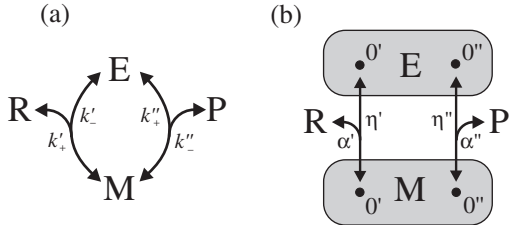

Fig. 4. A two-step, from the chemical point of view, enzymatic reaction. R and P stand for the reactant and the product, E stands for the free enzyme and M stands for the Michaelis complex. (a) The cycle performed by the enzyme, described in terms of conventional kinetics. (b) The scheme involving the intramolecular conformational transition dynamics of the enzyme. The multitudes of conformational transitions within E and M are represented by shaded boxes. Both component reactions are assumed to be gated by this dynamics. Notation of the rate constants and the transition probabilities between the gates is shown.

To determine for such a model the steady-state reaction flux per enzyme molecule:

$$J = [\dot{\mathrm{P}}]/[\mathrm{E}]_0 = -[\dot{\mathrm{R}}]/[\mathrm{E}]_0, \tag{4.1}$$

where $[\mathrm{E}]_0$ denotes the total concentration of the enzyme:

$$[\mathrm{E}]_0 = [\mathrm{E}] + [\mathrm{M}], \tag{4.2}$$

one has to know the steady-state occupation probabilities of the gates. These are to be calculated with the help of the technique just developed. On using Eq. (2.3) and the notation explained in Fig. 4(b) we have

$$\begin{aligned} J &= \alpha'[\mathrm{R}]\, p_{\mathrm{E}0'} - \eta' p_{\mathrm{M}0'} \\ &= \alpha'[\mathrm{R}]\, D_{0'}(\mathrm{E})\, \eta'' D_{0''}(\mathrm{M})\, D(\mathrm{S})^{-1} - \eta' D_{0'}(\mathrm{M})\, \alpha''[\mathrm{P}]\, D_{0''}(\mathrm{E})\, D(\mathrm{S})^{-1}. \end{aligned} \tag{4.3}$$

The diagrams are labelled by a letter corresponding to a given species, and the letter S denotes the total diagram containing E and M and the transitions between the gates as well. On using the detailed balance conditions

$$\eta' p^{\mathrm{eq}}_{\mathrm{M}0'} = \alpha'[\mathrm{R}]^{\mathrm{eq}}\, p^{\mathrm{eq}}_{\mathrm{E}0'}, \qquad \eta'' p^{\mathrm{eq}}_{\mathrm{M}0''} = \alpha''[\mathrm{P}]^{\mathrm{eq}}\, p^{\mathrm{eq}}_{\mathrm{E}0''} \tag{4.4}$$

we can rewrite the flux (4.3) as

$$J = \frac{\alpha'[\mathrm{R}]\, D_{0'}(\mathrm{E})\, \eta'' D_{0''}(\mathrm{M})}{D(\mathrm{S})} \left(1 - K^{-1} \frac{[\mathrm{P}]}{[\mathrm{R}]}\right), \tag{4.5}$$

where K is the equilibrium constant for the noncatalysed reaction:

$$K = [\mathrm{P}]^{\mathrm{eq}}/[\mathrm{R}]^{\mathrm{eq}}. \tag{4.6}$$

The denominator $D(\mathrm{S})$ is a sum of 10 kinds of directional diagrams presented in Fig. 5. After summing them up we find that the flux J can be written in the form

$$J = \frac{1 - e^{-\beta A}}{\tau_+ + \tau_- e^{-\beta A} + \tau_0 (K + e^{\beta A})^{-1}}, \tag{4.7}$$

where A denotes the thermodynamic force conjugate to J:[19]

$$A = \beta^{-1} \ln K \frac{[\mathrm{R}]}{[\mathrm{P}]} \tag{4.8}$$

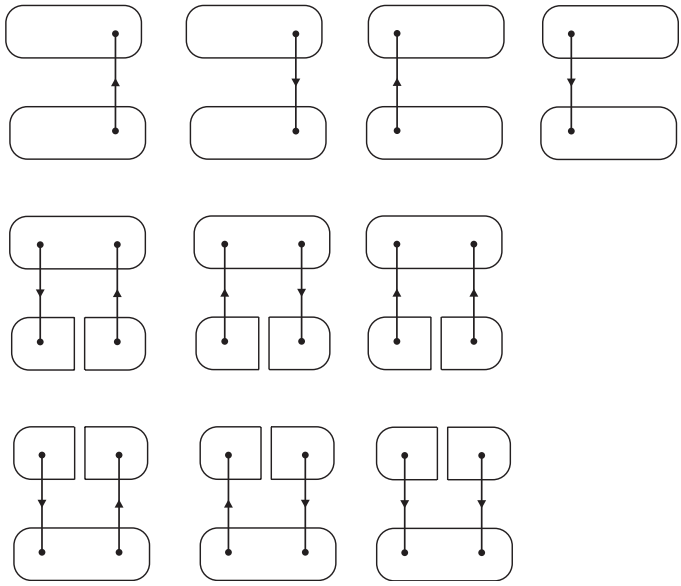

Fig. 5. Ten kinds of directional diagrams for the scheme of stochastic dynamics presented in Fig. 4(b). Only direct transitions between the gates are explicitely drawn. In the notation explained in Section 2, Eqs. (2.2), (2.5), and (2.11), for any subdiagram $\mathrm{N} = \mathrm{E}$ or M the full box with no exit gates counts as $D(\mathrm{N})$, the full box with one exit gate l as $D_l(\mathrm{N})$, the dissected box with one exit gate l and one entrance gate l' as $D_{l,l'}(\mathrm{N})$) and the dissected box with two exit gates l and l' and no entrance gate as $S_{l,l'}(\mathrm{N})$.

(β is the reciprocal temperature multiplied by the Boltzmann constant). In Eq. (4.7) we applied the chemical equation of state

$$[\mathrm{R}] = [\mathrm{R}]_0\,(1+Ke^{-\beta A})^{-1} \tag{4.9}$$

assuming that in the open reactor under discussion, the sum

$$[\mathrm{R}]_0 = [\mathrm{R}]+[\mathrm{P}] \tag{4.10}$$

remains constant.

The parameters $\tau_\pm$ have the meaning of the asymptotic flux periods. Indeed, for $\beta A \gg 1$ ($[\mathrm{R}]_0 = [\mathrm{R}]$), the flux $J \to \tau_+^{-1}$, whereas for $\beta A \ll -1$ ($[\mathrm{R}]_0 = [\mathrm{P}]$), the flux $J \to -\tau^{-1}$. The dependence of $\tau_\pm^{-1}$ on $[\mathrm{R}]_0$ was found to be of the conventional Michaelis–Menten form:[16]

$$\tau_\pm^{-1} = \frac{k_\pm [\mathrm{R}]_0}{K_\pm + [\mathrm{R}]_0}, \tag{4.11}$$

the expressions for the phenomenological parameters $k_\pm$ and $K_\pm$ we get are, however, unconventional. In the notation explained in Fig. 4(b), the reciprocal turnover numbers

$$k_+^{-1} = (k_+''^{\mathrm{eq}})^{-1} + \tau_{\mathrm{E}}(0'' \to 0') + \tau_{\mathrm{M}}(0' \to 0''), \tag{4.12}$$

$$k_-^{-1} = (k_-'^{\mathrm{eq}})^{-1} + \tau_{\mathrm{E}}(0' \to 0'') + \tau_{\mathrm{M}}(0'' \to 0'), \tag{4.13}$$

and the apparent dissociation constant

$$K_+ = K' k_+ [(k_+''^{\mathrm{eq}})^{-1} + (k_-'^{\mathrm{eq}})^{-1} + \tau_{\mathrm{M}}(0' \leftrightarrow 0'')], \tag{4.14}$$

K' being the actual dissociation constant:

$$K' = [\mathrm{R}]^{\mathrm{eq}}\,[\mathrm{E}]^{\mathrm{eq}}/[\mathrm{M}]^{\mathrm{eq}}. \tag{4.15}$$

The apparent dissociation constant K_- is related to K_+ by the Haldane equation:[16]

$$K_-/K_+ = (k_-/k_+)\,K. \tag{4.16}$$

The quantities

$$k_+''^{\mathrm{eq}} = (p_{\mathrm{M}0''}^{\mathrm{eq}}/P_{\mathrm{M}}^{\mathrm{eq}})\,\eta'', \qquad k_-'^{\mathrm{eq}} = (p_{\mathrm{M}0'}^{\mathrm{eq}}/P_{\mathrm{M}}^{\mathrm{eq}})\,\eta' \tag{4.17}$$

($P_{\mathrm{M}}^{\mathrm{eq}}$ denotes the equilibrium molar ratio of the enzyme-substrate complex M and p^{eq}'s denote the equlibrium occupation probabilities of the appropriate conformational substates) are the equilibrium (transition state theory) rate constants and τ_{E} and τ_{M} are the mean first-passage times between the specified gates within E and M, respectively (cf. notation (2.10) for the sum of the forward and backward mean first-passage times). The mean first passage times in Eqs. (4.12) to (4.14) are between the succeeding gates and not between the "typical" average states and the gates as in the full expression for the rate constant (3.7), thus the parameters $k_{\pm}$ and $K_{\pm}$ cannot be expressed in terms of the rate constants $k'_{\pm}$ and $k''_{\pm}$ describing the conventional kinetics presented in Fig. 4(a).

The parameter τ_0 determines the position of an inflection point on the flux-force functional dependence (4.7) and is related to the mean first-passage times between the gates within the free enzyme E:

$$\tau_0 = (K')^{-1}\,[\mathrm{R}]_0\,\tau_{\mathrm{E}}(0' \leftrightarrow 0''). \tag{4.18}$$

More complex (Haldane's) kinetics of enzymatic reaction[16] can be considered when replacing the single Michaelis complex M by the enzyme-reactant and the enzyme-product complexes combined by an additional gate representing explicitly the very catalysed covalent reaction (Fig. 6). On substituting $\tau_{\mathrm{M}}(0' \to 0'')$ and $\tau_{\mathrm{M}}(0'' \to 0')$ by expressions like (3.4), including the corresponding equilibrium rate constants, one reconstructs the formulae derived previously for the particular protein machine model of intramolecular dynamics.[9]

If the transition states of the component reactions compose a few conformational substates of different transition probabilities the total

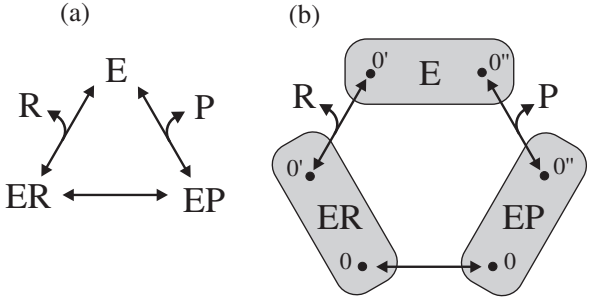

Fig. 6. A three-step, from the chemical point of view, enzymatic reaction. ER and EP stand for the enzyme-reactant and the enzyme-product complexes, respectively. (a) The conventional scheme. (b) The scheme involving the intramolecular conformational transition dynamics of the enzyme. The multitudes of conformational transitions within E, ER and EP are represented by shaded boxes. All component reactions are assumed to be gated.

steady state forward or backward reaction flux is a sum of several terms like (4.11) with different values of the apparent dissociation constant K_+ or K_-. However, this sum cannot have in general the Michaelis–Menten form. Consequently, the sufficient condition for the dynamically controlled enzymatic process to follow the Michaelis–Menten steady-state kinetics is gating the component binding-rebinding reactions. That a vast majority of enzymatic reactions actually obey the Michaelis–Menten law[16] is, when confronted with the proofs of the slow character of intramolecular protein dynamics mentioned at the begining, a strong argument for the gated mechanism of protein involving reactions, we assumed as the basis of all theoretical models considered.

5. TWO COUPLED ENZYMATIC REACTIONS

As the second application of our tool let us consider the case of great biological importance of two (for simplicity, unimolecular) reactions:

$$R_1 \leftrightarrow P_1 \qquad \text{and} \qquad R_2 \leftrightarrow P_2,$$

one being free energy-donating, e.g., ATP hydrolysis, and the other free energy-accepting, e.g., other substrate phosphorylation, or simulating a process of a substrate transfer through the membrane against the concentration gradient or translation of some cargo by a step along the microfilament or microtubule. Both reactions are catalyzed by the common enzyme which makes them thermodynamically coupled. If we shall refer as a *machine* to any physical system enabling two other physical systems to perform work on each other, such an enzyme appears a molecular machine that operates following controlled fluctuations in the isothermal conditions.

Four possible kinetic schemes can be devised on assuming one substrate-enzyme intermediate for each catalysed reaction: both reactions are coupled through the free enzyme E (Fig. 7(a)), both are coupled through the intermediate complex M (Fig. 7(b)), the intermediate complex for one reaction appears to be the free enzyme for the second reaction (Fig. 7(c)) and both reactions proceed as alternating half-reactions (Fig. 7(d)). The scheme from Fig. 7(a) applies, e.g., for substrate phosphorylation, that from Fig. 7(b) for molecular motors, and those from Figs. 7(c) and (d) for molecular pumps.[21] Further on we confine our attention only to the scheme (b) in Fig. 7; the reamaining schemes can be treated in a similar way. The multiconformational counterpart of this scheme is given in Fig. 8. Here, like in the scheme in Fig. 4(b), the multitudes of conformational transitions within two enzyme-one-substrate complexes E_1 and E_2 and the ternary complex M as well are represented by shaded boxes and the

assumption of gating is made. The scheme has an explicit symmetry: rotation by 180° changes the index 1 into 2 and vice versa.

In the steady state, with the molar concentrations of the reactants $[R_i]$ and products $[P_i]$ kept constant, there are two *operational* fluxes

$$J_i = [\dot{P}_i]/[E]_0 = -[\dot{R}_i]/[E]_0 \tag{5.1}$$

($i = 1, 2$), $[E]_0$ being the total concentration of the enzyme:

$$[E]_0 = [E_1] + [E_2] + [M], \tag{5.2}$$

and two conjugate thermodynamic forces

$$A_i = \beta^{-1} \ln K_i \frac{[R_i]}{[P_i]} \tag{5.3}$$

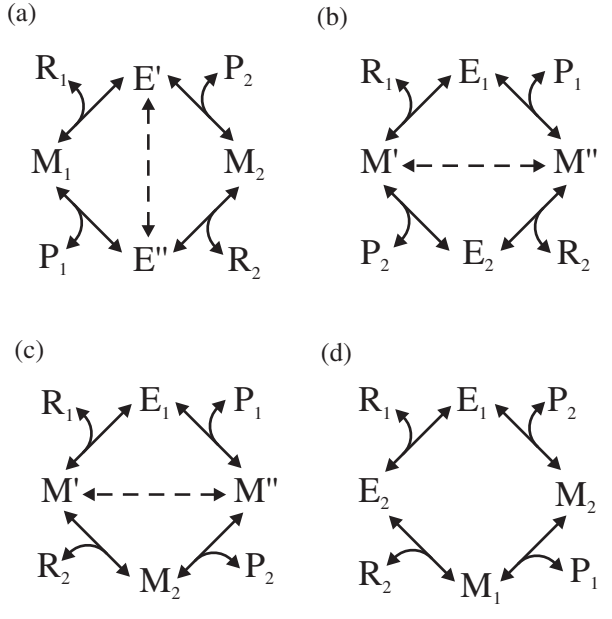

Fig. 7. Four possible coupling schemes of two reactions $R_1 \leftrightarrow P_1$ and $R_2 \leftrightarrow P_2$ by a common enzymatic complex. Broken line marks a possible direct transition with no substrate binding or release between two forms of enzyme or its complexes (the relative slippage of two enzymatic cycles).

acting in the system.[19] The quantities K_i denote the equilibrium constants for the non-catalysed reactions:

$$K_i \equiv \frac{[\mathrm{P}_i]^{\mathrm{eq}}}{[\mathrm{R}_i]^{\mathrm{eq}}}. \tag{5.4}$$

Thermodynamic forces measure the distance from the equilibrium, at which they vanish. The sum

$$J_1 A_1 + J_2 A_2 = \Phi \geqslant 0, \tag{5.5}$$

nonnegative on the behalf of the second law of thermodynamics, determines the dissipation flux. The free energy transduction is realized if the products $J_1 A_1$ and $J_2 A_2$, having the meaning of the *power input* and the *power output*, are of different signs. If we assume the force A_2 to be negative, reaction 2, in the absence of reaction 1, proceeds from P_2 to R_2. It is the occurrence of reaction 1 that can drive reaction 2 against the conjugate force A_2.

The *efficiency* of the machine is the ratio

$$\eta \equiv \frac{-J_2 A_2}{J_1 A_1} = \frac{J_1 A_1 - \Phi}{J_1 A_1} = 1 - \frac{\Phi}{J_1 A_1}. \tag{5.6}$$

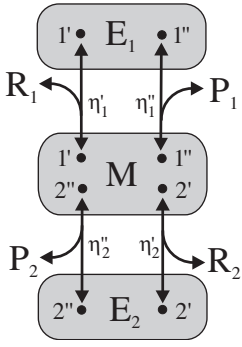

Fig. 8. A scheme of two coupled enzymatic reactions involving the intramolecular conformational transition dynamics of the enzyme. It is the multiconformational counterpart of the scheme (b) in Fig. 7. The slippage takes place within a single common form of the ternary complex M. The multitudes of conformational transitions within E_1, E_2 and M are represented by shaded boxes. All the component reactions are assumed to be gated. Only the notation of the unimolecular transition probabilities between the gates is shown; values of the corresponding probabilities of bimolecular transitions in the opposite direction, proportional to the concentrations $[\mathrm{R}_i]$ or $[\mathrm{P}_i]$, are related by the detailed balance condition.

In general, the flux J_2 can differ from the flux J_1 beacause of a possible *slippage* of the corresponding cycles when passing through the substates in M (cf. Fig. 8 as well as Figs. 7(a)–(c)). The measure of the slippage is a deviation of the *degree of coupling* of both fluxes

$$\epsilon \equiv \frac{J_2}{J_1} \tag{5.7}$$

from unity. The quantity (5.7) can be both smaller or larger than unity. In terms of the degree of coupling the eficciency (5.6) can be rewritten as a product

$$\eta = -\frac{A_2}{A_1}\epsilon. \tag{5.8}$$

The operational fluxes (5.1) for the model stated are determined by the steady-state occupation probabilities of appropriate gates. These are to be calculated with the help of the technique described in detail in Section 2. There are 63 kinds of directional diagrams that have to be taken into account. Five of them, contributing to the occupation probability of the gate $E_1 1''$, are shown in Fig. 9.

The flux-force relations which we have found for the scheme of two coupled reactions given in Fig. 8 are of the same functional form as the flux-force relation for separate reactions, Eq. (4.7):

$$J_i = \frac{1 - e^{-\beta(A_i - A_i^{\mathrm{st}})}}{\tau_{+i} + \tau_{-i} e^{-\beta(A_i - A_i^{\mathrm{st}})} + \tau_{0i}(K_i + e^{\beta A_i})^{-1}} \tag{5.9}$$

($i = 1, 2$). Now, however, the parameters τ_{+i}, τ_{-i} and τ_{0i} depend yet on another force and their dependence on the mean first-passage times, transition state theory reaction rates and the concentrations of the substrates is much more complex. Moreover, there are aditionanal parameters A_i^{st}, determining the non-zero values of *stalling forces*, for which only the fluxes J_i vanish. For the flux J_i to be a unique function of the force A_i we assumed that the total concentrations of the reactants and the products of each kind

$$[\mathrm{R}_i]_0 = [\mathrm{R}_i] + [\mathrm{P}_i] \tag{5.10}$$

remain constant.

The dependence $J_i(A_i)$, Eq. (5.9), is strictly increasing with an inflection point and two asymptotes (Fig. 10). As we have said the free energy

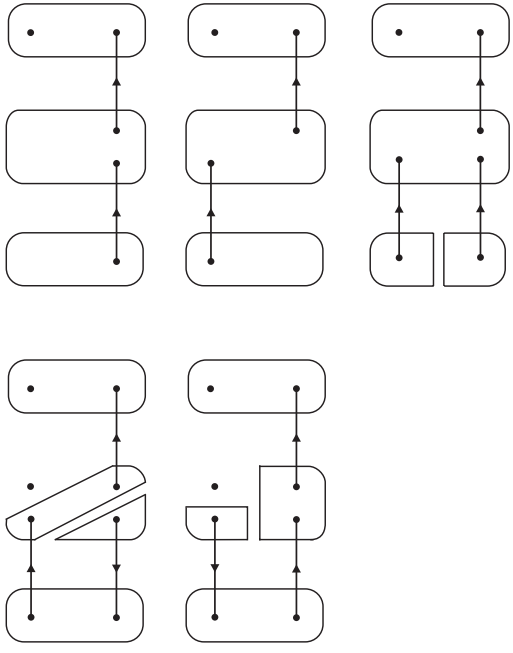

Fig. 9. Five kinds of directional diagrams contributing to the occupation probability of the gate $E_1 1'$ in the scheme presented in Fig. 8. In the notation explained in Section 2, cf. Eqs. (2.11) and (2.18), for a subdiagram $N = E_1$, E_2 or M, the full box with one exit gate l counts as $D_l(N)$, the dissected box with two exit gates l, l' and no entrance gate as $S_{l,l'}(N)$, and the dissected box with two exit gates l and l', the former belonging to the same sub-box as the entrance gate l'', as $S_{l(l''),l'}(N)$ (the fourth gate in the case of M may belong to either sub-box).

transduction takes place if one of the fluxes, say J_2, is of the opposite sign to its conjugate force, A_2. From Eq. (5.9) it follows that this condition holds when the corresponding stalling force A_2^{st} is negative. The dependence $J_2(A_2)$ in the range $A_2^{st} \leqslant A_2 \leqslant 0$ can be convex, concave or involving an inflection point as well.

We are not going to give the full expressions for the prarameters τ_{+i}, τ_{-i} and τ_{0i} but formula which we have obtained for the degree of coupling (5.7) is not that complex and it is worth quoting. We shall write it down in the form

$$\epsilon = \frac{T_1(A_1)[1 - e^{-\beta(A_2 - A_2^{st})}]}{T_2(A_2)[1 - e^{-\beta(A_1 - A_1^{st})}]}. \tag{5.11}$$

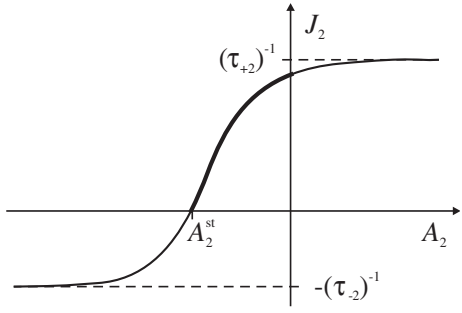

Fig. 10. The character of the functional dependence of the output flux J_2 vs force A_2. Only when the stalling force A_2^{st} is negative, the output flux has the opposite sign to its conjugate force and the process of the free energy transduction takes place. The $J_2(A_2)$ dependence in this range is marked with the bold line.

The quantity $T_1(A_1)$, of the dimension of time, is given by the equation

$$\begin{aligned} T_1(A_1) \equiv\ & (k_{+1''}^{eq})^{-1} + \tau_M(\{1', 2''\} \leftrightarrow 1'') \\ & + [(k_{-1'}^{eq})^{-1} + \tau_M(1' \leftrightarrow \{1'', 2''\})]\, e^{-\beta A_1} \\ & + \tau_{E_1}(1' \leftrightarrow 1'')\, ([M]^{eq}/[E_1]^{eq})\, (K_1 + 1)\, (K_1 + e^{\beta A_1})^{-1}, \end{aligned} \tag{5.12}$$

where the transition state theory unimolecular rate constants

$$k_{-1'}^{eq} = (p_{M1'}^{eq}/P_M^{eq})\, \eta_1', \qquad k_{+1''}^{eq} = (p_{M1''}^{eq}/P_M^{eq})\, \eta_1'' \tag{5.13}$$

(cf. the explanations to Eqs. (4.17), the sign + or − in the lower index is added depending on whether a given reaction proceeds in a counterclockwise or a clockwise direction) and τ_M and τ_{E_1} denote the mean first-passage times back and forth between the specified gates (possibly alternative, cf. end of Section 2) within M and E_1, respectively. Mutual permutation of 1 with 2, corresponding to the rotation of the scheme in Fig. 8 by 180°, results in a similar formula for the quantity $T_2(A_2)$.

The quantity $T_1(A_1)$ determines the value of the stalling force A_2^{st}, which is the function of A_1:

$$\beta A_2^{st} = \ln\left[1 + \frac{\tau_M(1' \leftrightarrow \{1'', 2'\}) - \tau_M(1' \leftrightarrow \{1'', 2''\})}{T_1(A_1)}\,(e^{-\beta A_1} - 1)\right] \tag{5.14}$$

(if $A_2 = A_2^{st}$ the degree of coupling $\epsilon = 0$). Mutual permutation of 1 with 2 results in a similar formula for the stalling force A_1^{eq} determined by $T_2(A_2)$ (if $A_1 = A_1^{st}$ the reciprocal degree of coupling $\epsilon^{-1} = 0$).

We do not discuss the conditions for the maximum efficiency of the free-energy trasduction process as even in the linear approximation of the flux-force relations (which is a bad approximation in usual physiological and laboratory conditions) the formulae for the values of forces maximizing the efficiency are very complex.[22] Anyhow, the conditions for the maximum efficiency and those for the maximum power output contradict each other. The machine is the more efficient the lower is free energy dissipation, i.e., the slower it works. But the slower it works the lower is its power output.

However, not always the maximum efficiency or the maximum power output are the optimum from the point of view of living organism. Very often the power output of biological machines equals simply to zero, i.e., the output forces stall the machines. It can be the case of molecular motors and molecular pumps as well. Muscles of a man sustaning a big load do not perform any work (physiologists use not a quite logical term "isometric contraction" of muscle) but, of course, ATP is consumed in some amounts. The intracellular concentration of Ca^{2+} is kept at a very low level to avoid association with phosphate ions P_i, whereas that of K^+, conversely, at a very high level to secure the appropriate value of the plasma membrane resting potential.[21] It is due to the ATP hydrolysis by the corresponding pumps that the ions do not flow into or out of the cell despite the concentration differences. All cases considered are similar to that of a car which keeps standing at the inclined slope with its wheels constantly rotating and slipping.

State of the zero power output is advantageous for the organism because it can be maintained irrespective of environmental changes (homeostasis). The attainable range of variability of the force stalling the machine is, however, limited. The dependence found, Eq. (5.14), of the negative stalling force $-A_2^{st}$ (we assumed $A_2 \leqslant 0$ for the free energy transduction to accomplish) vs the force A_1 is strictly increasing but it saturates both for very large positive and very large negative values of A_1. The force A_2 of a value from outside the range determined is no more able to stall the machine. For small values of βA_1, the $-A_2^{st}$ vs A_1 dependence, Eq. (5.14), can be linearized:

$$-A_2^{st} = \frac{[\tau_M(1' \leftrightarrow \{1'', 2'\}) - \tau_M(1' \leftrightarrow \{1'', 2''\})]\, A_1}{(k_{+1''}^{eq})^{-1} + (k_{-1'}^{eq})^{-1} + \tau_M(1' \leftrightarrow 1'') + ([M]^{eq}/[E_1]^{eq})\, \tau_{E_1}(1' \leftrightarrow 1'')}. \tag{5.15}$$

A similar relation can be derived for the $-A_1^{st}$ vs A_2 dependence with the proportionality coefficient to be gotten from Eq. (5.15) after mutual

permutation of 1 with 2. In both cases the relation (2.19) ensures the proportionality coefficient to have a value between 0 and 1.

The assumption of the positive values of βA_1 and the negative values of βA_2 is easy satisfied if

$$K_1 \gg e^{\beta A_1} > 1 \qquad \text{and} \qquad K_2 \ll e^{\beta A_2} < 1 \tag{5.16}$$

(cf. Eq. (5.3)), i.e., the machine is highly asymmetrical. If, additionally, we assume that the mean first-passage times in M, related to the realization of the reaction $\mathrm{R}_1 \leftrightarrow \mathrm{P}_1$ and $\mathrm{R}_2 \leftrightarrow \mathrm{P}_2$ are much longer than those not related to it:

$$\tau_{\mathrm{M}}(1' \leftrightarrow \{1'', 2''\}) \ll \tau_{\mathrm{M}}(\{1', 2''\} \leftrightarrow 1'') \approx \tau_{\mathrm{M}}(1' \leftrightarrow 1'') \tag{5.17}$$

and

$$\tau_{\mathrm{M}}(\{1', 2'\} \leftrightarrow 2'') \ll \tau_{\mathrm{M}}(2' \leftrightarrow \{1', 2''\}) \approx \tau_{\mathrm{M}}(2' \leftrightarrow 2'') \tag{5.18}$$

(cf. Eq. (2.19)), Eq. (5.11) is simplified to

$$\epsilon = \frac{[\tau_{1''} + \tau_{\mathrm{M}}(1' \leftrightarrow 1'')]\, e^{\beta A_2} - [(k^{\mathrm{eq}}_{-1'})^{-1} + \tau_{\mathrm{M}}(1' \leftrightarrow 1'')]\, e^{-\beta A_1} - \tau_{1''}}{[(k^{\mathrm{eq}}_{+2''})^{-1} + \tau_{\mathrm{M}}(2' \leftrightarrow 2'')]\, e^{\beta A_2} - [\tau_{2'} + \tau_{\mathrm{M}}(2' \leftrightarrow 2'')]\, e^{-\beta A_1} + \tau_{2'}} \tag{5.19}$$

and the expressions for the stalling forces A_2^{st} and A_1^{st} to

$$\beta A_2^{\mathrm{st}} = \ln \frac{[(k^{\mathrm{eq}}_{-1'})^{-1} + \tau_{\mathrm{M}}(1' \leftrightarrow 1'')]\, e^{-\beta A_1} + \tau_{1''}}{\tau_{1''} + \tau_{\mathrm{M}}(1' \leftrightarrow 1'')} \tag{5.20}$$

and

$$\beta A_1^{\mathrm{st}} = -\ln \frac{[(k^{\mathrm{eq}}_{+2''})^{-1} + \tau_{\mathrm{M}}(2' \leftrightarrow 2'')]\, e^{\beta A_2} + \tau_{2'}}{\tau_{2'} + \tau_{\mathrm{M}}(2' \leftrightarrow 2'')}, \tag{5.21}$$

where we have introduced notation

$$\tau_{1''} \equiv (k^{\mathrm{eq}}_{+1''})^{-1} + ([\mathrm{M}]^{\mathrm{eq}}/[\mathrm{E}_1]^{\mathrm{eq}})\, \tau_{\mathrm{E}_1}(1'' \leftrightarrow 1') \tag{5.22}$$

and

$$\tau_{2'} \equiv (k^{\mathrm{eq}}_{-2'})^{-1} + ([\mathrm{M}]^{\mathrm{eq}}/[\mathrm{E}_2]^{\mathrm{eq}})\, \tau_{\mathrm{E}_2}(2' \leftrightarrow 2''). \tag{5.23}$$

Note breaking the symmetry with respect to the permutation of 1 with 2, which results from the assumption of different signes of βA_1 and βA_2.

Usually, biological molecular machines operate under the excess of ATP,[21] i.e., subsystem 1 is far from equilibrium, $\beta A_1 \gg 1$, so we can neglect the term $e^{-\beta A_1}$ in the flux-force relations (5.9) and the flux J_1 is reduced to $(\tau_{+1})^{-1}$. In such conditions, the approximation just discussed simplifies not only the formula for the degree of coupling ϵ, Eq. (5.19), but also the formulae for the parameters τ_{+2}, τ_{-2} and τ_{02}, related to τ_{+1}, which appear now to be worth quoting:

$$\tau_{+2} = \frac{[\mathrm{R}_1]^{\mathrm{eq}}\,[\mathrm{E}_1]^{\mathrm{eq}}}{[\mathrm{M}]^{\mathrm{eq}}}\,([\mathrm{R}_1]_0\,k^{\mathrm{eq}}_{+2''})^{-1} + ([\mathrm{R}_2]_0\,k^{\mathrm{eq}}_{+2'})^{-1} + K_2^{-1}([\mathrm{R}_2]_0\,k^{\mathrm{eq}}_{-2''})^{-1}$$
$$+ \frac{\tau_{\mathrm{M}}(2' \leftrightarrow 2'')}{\tau_{\mathrm{M}}(1' \leftrightarrow 1'')}\left[\frac{[\mathrm{E}_2]^{\mathrm{eq}}}{K_2[\mathrm{M}]^{\mathrm{eq}}}\,(k^{\mathrm{eq}}_{+1''})^{-1} + ([\mathrm{R}_1]_0\,k^{\mathrm{eq}}_{+1'})^{-1} + \tau_{\mathrm{E}_1}(1'' \to 1')\right]$$
$$+ \tau_{\mathrm{E}_2}(2'' \to 2'), \tag{5.24}$$

$$\tau_{-2}e^{\beta A_2^{\mathrm{st}}} = \frac{[\mathrm{R}_1]^{\mathrm{eq}}\,[\mathrm{E}_1]^{\mathrm{eq}}}{[\mathrm{M}]^{\mathrm{eq}}}\,([\mathrm{R}_1]_0 k^{\mathrm{eq}}_{-2'})^{-1} + K_2([\mathrm{R}_2]_0\,k^{\mathrm{eq}}_{+2'})^{-1} + ([\mathrm{R}_2]_0\,k^{\mathrm{eq}}_{-2''})^{-1}$$
$$+ \tau_{\mathrm{E}_2}(2' \to 2''), \tag{5.25}$$

and

$$\tau_{02} = \frac{[\mathrm{R}_1]^{\mathrm{eq}}\,[\mathrm{E}_1]^{\mathrm{eq}}}{[\mathrm{R}_1]_0\,[\mathrm{E}_2]^{\mathrm{eq}}}\,\tau_{\mathrm{E}_2}(2' \leftrightarrow 2''). \tag{5.26}$$

We approximated the equilibrium constant K_1 by the ratio $[\mathrm{R}_1]_0/[\mathrm{R}_1]^{\mathrm{eq}}$. In the limit $\beta A_1 \gg 1$, because the degree of coupling ϵ does not depend on $[\mathrm{R}_1]_0$, both J_1 and J_2 show the same Micheelis–Menten dependence on $[\mathrm{R}_1]_0$, usually denoting the ATP concentration:

$$J_1 = \epsilon^{-1}J_2 = \frac{k_+[\mathrm{R}_1]_0}{K_+ + [\mathrm{R}_1]_0}. \tag{5.27}$$

We do not quote the general formulae for the parameters k_+ and K_+ which can be easy found from Eqs. (5.9) and (5.20), and the formulae for the parameters τ_{+2}, τ_{-2} and τ_{02}.

Further approximations depend on a particular problem one is dealing with at the moment. In the next Section we consider in more detail the case of actomyosin molecular motor.

6. THEORY OF MECHANOCHEMICAL COUPLING IN ACTOMYOSIN MOLECULAR MOTOR

The scheme from Fig. 8 studied in the previous Section is in fact a multiconformational counterpart of the Lymn–Taylor–Eisenberg model of a mechanochemical cycle of the actomyosin molecular motor.[23–27] Contrary to kinesin[28,29] and the F_1 portion of ATP synthase[30]—two motor molecules being recently the subject of extensive theoretical studies, the myosin molecule, like nucleic acid polymerases,[31,32] is capable to act in a non-cooperative manner. The actomyosin motor consists of a single myosin head (some 1200 amino acid recidues) moving along the thin actin filament.[21,27] The Lymn–Taylor–Eisenberg kinetic scheme indicates how the ATPase cycle of myosin is related to a detached, weakly-attached and strongly-attached states of the myosin head to the actin filament (Fig. 11). Both the substrate and the products of the catalysed reaction bind to and rebind from the myosin in its strongly attached state whereas the very reaction takes place either in the weakly-attached or in the detached state. Only completion of a whole cycle with the ATP hydrolysis realized in the detached state of the myosin molecule results in the directed motion along the actin track; the ATP hydrolysis in the weakly bound state alone is ineffective (the slippage).

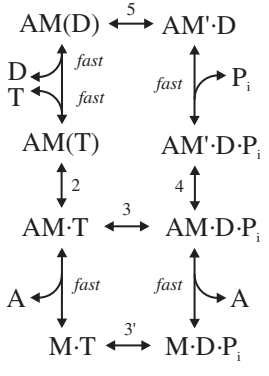

Fig. 11. Lymn–Taylor–Eisenberg kinetic model of mechanochemical cycle of the actomyosin motor in the version of Ma and Taylor[25] with a few distinguished conformational states of myosin. M denotes the myosin head, A the actin filament, T, D and P_i stand for ATP, ADP and inorganic phosphate, respectively. The original labelling of the reaction steps used by those authors is indicated. The values of particular rate constants are $k_{+2} = 1.8\ k_{-2} \geqslant 1000\ s^{-1}$, $k_{+3} \approx k_{-3} \leqslant 150\ s^{-1}$, $k_{+3'} = 150\ s^{-1}$, $k_{-3'} < 15\ s^{-1}$, $k_{+4} = 2.2\ k_{-4} = 140\ s^{-1}$, and $k_{+5} = 500\ s^{-1}$ (see also a thermodynamic study by Zhao and Kawai[26] and a compilation by Howard[27]). The sign + or − in the lower index denotes whether a given reaction proceeds in a counterclockwise or a clockwise direction. The binding-rebinding reaction steps are much faster.

Following the swinging lever-arm idea,[33] the motor force is generated in the strongly-attached state by a rotational motion of a catalytic domain of the myosin head (some 650 amino acid residues) relative to a regulatory "lever-arm" domain (some 550 residues) further on connected by a limp α-helical thread to a cargo (the thick filament in the case of the muscle sarcomere). The swinging lever-arm picture has strong grounds in the motility assays,[34, 35] the X-ray crystallography,[36–39] the electron micrography,[40] time-resolved electron cryomicroscopy,[41] observations of hyperfine structure of EPR spectra,[42, 43] fluorescence polarization,[44, 45] and fluorescence resonance energy transfer.[46–48]

No agreement has been reached yet on the very mechanism of the mechanochemical coupling. Presumably, much of the superfluous discussion on this topic results from the fact that authors often do not clearly state which notion of the force they have in mind: that on the micro-, meso- or macroscopic level? The force in the Newtonian sense can be defined only on the *microscopic level* of motion of individual atoms. This is the subject of molecular dynamics and will not be considered here. The force exerted by a motor on a track, always balanced by the Brownian and the friction forces, has a meaning on the *mesoscopic level* of stochastic dynamics of a single motor macromolecule. Otherwise, the external load acts on a statistical ensemble of motor molecules composing the sarcomere or the whole muscle and can be directly defined only on the *macroscopic level* of irreversible thermodynamics. A matter of argument is how to include the external load on the mesoscopic level of the single molecule stochastic dynamics.

Following Hill,[19] the force exerted by individual molecules is a strictly molecular property, not dependent on macroscopic external constraints such as the load discussed. Thus this load, in the steady state simply balancing the mean force exerted by the ensemble of all motor molecules, can be only a property of the organization of the statistical ensemble. In particular, the load influences the number of myosin heads bound to the actin filament.[49] Other authors,[50] on the contrary, consider a macroscopic force as acting on individual molecules and changing the free energies of their particular conformational states, thus the probabilities of the corresponding stochastic transitions. All thermal ratchet models take into account the external load, either as a constat quantity[51–53] or as a variable depending on a particular conformational substate of the motor molecule.[54] In our opinion, however, these models apply directly *only* to single molecules, e.g., myosin sliding over an actin filament held in laser traps in the motility assay[34] or F_1 motor in ATP synthase.[30] In both cases the position of the motor, thus the force acting by or on it, has no thermodynamic, i.e., macroscopic meaning.

A crucial argument for the proper treatment of the load in the thermodynamic sense comes from the recent EPR studies by Baker *et al.*[42, 43] These authors distinguished only two discrete orientations of the myosin lever-arm domain, probably ordered by interactions with the core of the myosin thick filament. Changes of the external load in the isometric conditions, combined with the appropriate changes of the inorganic phosphate P_i concentration, appeared to lead to no changes in the distribution of both biochemical and orientational states of the myosin heads. The authors conclude that the load does not influence the conformational states of individual myosin heads and propose to explain the observation with the help of simultaneous changes of equilibria of the actin filament binding and the phosphate P_i releasing reactions.[55] This explanation is based on a rather restrictive assumption that in the isometric muscle, when the ATPase and mechanical cycles compensate each other, the concentrations of myosin heads attached to and detached from the actin filament are equal. If we reject this assumption and treat both cycles in arbitrary conditions independently, it will be sufficient to determine the effect of the load in terms of changes of the binding free energy to actin filament before and after translation by a unit step. It should be noted that these changes, being a measure of the departure from equilibrium, must not be related to changes of conformational free energies as in ref. 50, making use of the detailed balance condition, thus, contrary to the very authors, we consider their observation as confirming and not contradicting the Hill's point of view.

The changes of the binding free energy can be expressed as the changes of the effective rather than actual concentrations of the actin filament before and after translation. As a consequence, the actomyosin motor can be effectively treated as a usual chemo-chemical machine. We assume such an approach in the present paper. However, we consider the kinetic scheme in Fig. 11 to be insufficient for the proper description of the actomyosin mechanical cycle. Stochastic dynamics of individual myosin heads needs two distinct time scales, the fast one, of internal molecular vibrations, and the slow one, of conformational transitions. It is the averaging over vibrational degrees of freedom that leads to purely stochastic transitions between conformational substates of the well-defined free energy levels. Following what we said in the Introduction the number of such defined conformational substates appears to be much larger than that specified in Fig. 11.

Numerous experiments indicate considerable conformational mobility of the myosin head. Fluorescence polarization data show an essential increase of the dispersion of the lever-arm domain tilt angle relative to the actin filament axis during the change from rigor to relaxed physiological states of especially prepared muscle.[45] A local, internal conformational

disorder on the nanosecond time scale was observed when analysing the hyperfine splitting of EPR signal of a nitrooxide spin label.[56] A global, orientational disorder of the catalytic domain relative to both the actin filament and the lever-arm domain was observed in the microsecond time scale using the saturation transfer EPR[57, 59] and detection of fluorescence polarization of a single molecule.[44] The orientational disorder on the milisecond time scale was observed by the parallel studies of stopped-flow fluorescence and time-resolved electron cryomicroscopy.[41] Following many investigators[42, 57, 58] the "power stroke" is in fact a conformational disorder to order transition. A multitude of conformational states corresponding to this disorder has to be taken into account in the kinetic scheme.

To determine the force exerted by the myosin head on the actin filament, one usualy considers a quasi-continuum of conformational substates labeled with the help of a one-dimensional variable characterizing the position of a given fragment of the myosin head relative to a fixed point on the actine filament. The force is a negative derivative of the free energy with respect to this variable.[19, 49, 51–53] However, a possibility of the orientational motion of the catalytic domain relative to either the actin filament or the lever-arm domain indicates that the stochastic dynamics of conformational transitions in the actomyosin motor is much more complex than one-dimensional diffusion. In fact, both the X-ray crystallography[39] and the study of cross-linking between two thiols Cys-522 and Cys-707[60] or Cys-697 and Cys-707[61] show that bonding of ATP results in melting the SH1-SH2 helix, crucial for the myosin head rigidity. Several important for binding, flexible surface loops are not seen in the X-ray diffraction at all.[36–39]

As we have already told the scheme from Fig. 8 is exactly a multiconformational counterpart of the Lymn–Taylor–Eisenberg model, Fig. 11. The state E_1 represents the myosin-ADP complex strongly attached to the actin filament, the state M–the myosin-ATP or $ADP \cdot P_i$ complex weakly attached, and the state E_2, the latter complex detached from the actin filament. In physiological and most of experimental conditions, in the presence of creatine phosphate/creatine kinase system, the ADP concentration is few orders of magnitude lower than the ATP concentration[21] thus, for the fixed ADP concentration, the ATP hydrolysis can be treated effectively as a unimolecular reaction

$$R_1 \leftrightarrow P_1,$$

where R_1 is ATP and P_1 is the inorganic phosphate P_i. We have already mentioned that also physical motion can be treated as a unimomolecular reaction

$$R_2 \leftrightarrow P_2,$$

R_2 denoting the actin filament before translation and P_2, the actin filament after translation by a step (presence of the the load changes effective concentrations $[R_2]$ and $[P_2]$). As a consequence, the motor appears a chemo-chemical machine, enzymatically coupling two unimolecular reactions, a free energy-donating one and a free energy-accepting one.

All the binding-rebinding reactions are assumed to be gated, i.e., take place only in certain conformational substates (or small groups of such substates) of the myosin head. Figure 12, constructed on the basis of the results reported in the majority of the already cited experimental studies, mainly the X-ray crystallography,[36–39] characterizes schematically all the four gates denoted in Fig. 8 as 1′, 1″, 2′, and 2″.

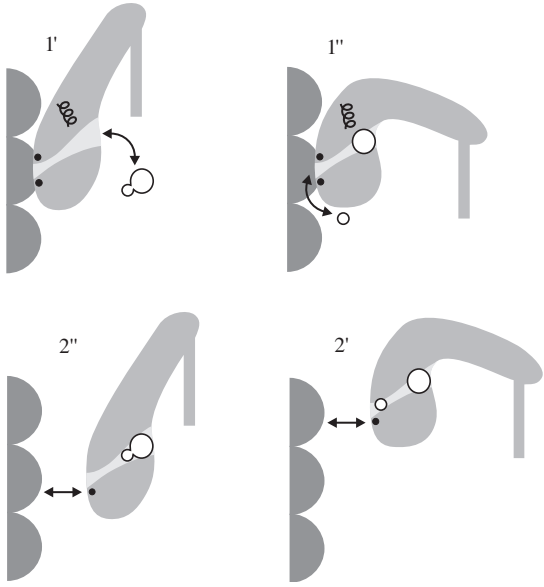

Fig. 12. Characteristics of four conformational substates of the myosin head being the gates for the four bimolecular binding-rebinding reactions in scheme presented in Fig. 8. In the state E_1 the strong attachement of the myosin head to the actin at two sites (the black dots) makes the nucleotide pocket (weakly shaded) relatively rigid. The SH1-SH2 helix transmits the motion of the lever-arm domain onto the pocket shape, which in the substate 1′ enables binding-rebinding the ATP molecule (two joined circles) and in the substate 1″, the P_i molecule (a smaller circle). In the detached state E_2 the SH1-SH2 helix is melted. For the myosin head to attach weakly (at one site) to the actin, an appropriate surface loop (the single black dot) has to assume an adequate shape, different for the nucleotide being non-hydrolysed (the substate 2″) or hydrolysed (the substate 2′). This can but need not be related to the position of the lever-arm domain. Here we assumed that these positions coincide with the corresponding positions in the E_1 state.

A consequence of the low concentration of ADP is a very large value of the equilibrium constant K_1 for the effectively unimolecular reaction of ATP hydrolysis. Conversely, because the structure of the actomyosin motor is highly asymmetric and effects of the same load, when applied in the opposite directions, differ very much, we assume the value of the equilibrium constant K_2 to be very small, the effective equilibrium concentration of P_2 being much lower than that of R_2. Thus, the conditions (5.16) are satisfied and it is easy for the force A_1 to be positive and for the force A_2, negative (but not the other way round!).

In the case of the actomyosin motor the flux-force dependence $J_2(A_2)$ is concave[62] which means (cf. Fig. 10) that

$$\tau_{+2} \ll \tau_{-2} e^{\beta A_2^{\mathrm{st}}}. \tag{6.1}$$

On neglecting τ_{+2} and assuming $K_2 = 0$ in Eq. (5.9) for $i = 2$ we get the functional dependence

$$J_2(A_2) = \frac{e^{\beta A_2} - e^{\beta A_2^{\mathrm{st}}}}{\tau_{-2} e^{\beta A_2^{\mathrm{st}}} + \tau_{02}} = J_2(0) \frac{e^{\beta A_2} - e^{\beta A_2^{\mathrm{st}}}}{1 - e^{\beta A_2^{\mathrm{st}}}}, \tag{6.2}$$

where $J_2(0)$ is the value of the flux J_2 for $A_2 = 0$, i.e., in the absence of the load. Function (6.2) describes experimental behaviour equally well as the phenomenological A. V. Hill's hyperbolic dependence[62] and in Fig. 13 we show how it fits the data of He *et al.*[62] for the sarcomere shortening velocity. The fitted values of the negative stalling force in $k_B T$ units, $-\beta A_2^{\mathrm{st}}$, we have got are much larger than 1. As a consequence, $e^{\beta A_2^{\mathrm{st}}}$ is small and the flux-force dependence $J_2(A_2)$ for the actomyosin motor can be simplified even more:

$$J_2(A_2) = J_2(0)\, e^{\beta A_2}. \tag{6.3}$$

Satisfaction of the inequalities (5.16) indicates that the approximations made at the end of the previous Section are, in the present case, justified. If, additionally, we take into account that the times of the bimolecular steps, described by the reciprocal transition state theory rate constants $(k^{\mathrm{eq}})^{-1}$, are negligibly small (cf. the caption of Fig. 11), the expressions (5.20) and (5.21) for the stalling forces A_2^{st} and A_1^{st} are simplified to

$$\beta A_2^{\mathrm{st}} = \ln \frac{e^{-\beta A_1} + c_1}{1 + c_1} \tag{6.4}$$

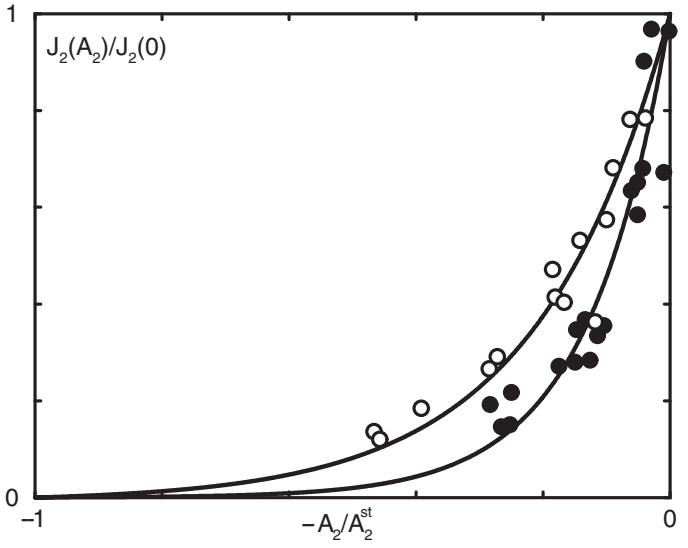

Fig. 13. Fit of Eq. (6.2) to the data of He *et al.*,[62] Fig. 3, for the sarcomere shortening velocity. The black circles correspond to the slow fibers and the white circles, to the fast 2A fibers in the terminology of those authors. The fitted values of the negative stalling force in k_BT units, $-\beta A_2^{st}$, were found to be equal 4.8 and 7.9 for the slow and the fast fibers, respectively.

and

$$\beta A_1^{st} = -\ln \frac{e^{\beta A_2} + c_2}{1 + c_2}, \tag{6.5}$$

where the parameters c_1 and c_2 denote the ratios

$$c_1 \equiv \frac{[\mathrm{M}]^{eq}\, \tau_{\mathrm{E}_1}(1' \leftrightarrow 1'')}{[\mathrm{E}_1]^{eq}\, \tau_{\mathrm{M}}(1' \leftrightarrow 1'')} \tag{6.6}$$

and

$$c_2 \equiv \frac{[\mathrm{M}]^{eq}\, \tau_{\mathrm{E}_2}(2' \leftrightarrow 2'')}{[\mathrm{E}_2]^{eq}\, \tau_{\mathrm{M}}(2' \leftrightarrow 2'')}, \tag{6.7}$$

respectively. In Fig. 14 we show how the function of the form (6.4) fits the experimental data of Pate *et al.*[63] The maximum value of 10.0 of the negative stalling force in k_BT units, $-\beta A_2^{st}$, is comparable to the values of 4.8 and 7.9 determined for other samples from the flux-force dependence, Fig. 13. In the linear range the negative stalling force $-\beta A_2^{st}$ was found to

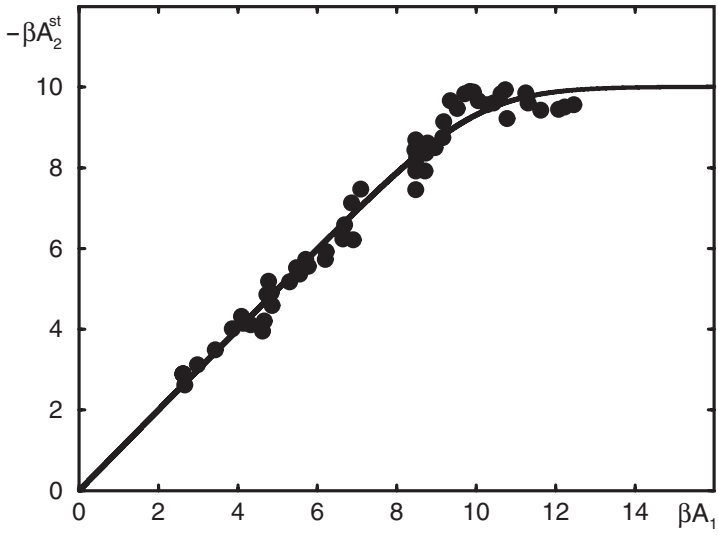

Fig. 14. Fit of Eq. (6.4) to the data of Pate *et al.*,[63] Fig. 6. We have assumed that the ratio of the concentrations of ADP and ATP were fixed constant during the experiment so that the concentration of inorganic phosphate P_i determines directly the force βA_1 in $k_B T$ units. The proportionality coefficient between the negative stalling force $-\beta A_2^{st}$ and the force βA_1 in the linear range was found to equal unity with the accuracy better than 1 %. The maximum negative stalling force $-\beta A_2^{st}$ in $k_B T$ units was fitted to be equal 10.0, which corresponds to the value of the ratio c_1 to be 0.45×10^{-4}.

equal the force βA_1 with a high accuracy, which agrees with the small value of the parameter $c_1 = 0.45 \times 10^{-4}$ corresponding to the maximum value of the negative stalling force. We consider that the interpretation of the experimental data in terms of Eq. (6.4) is more correct than in terms of the formulae derived under the assumption of proximity to equlibrium.[63]

Far from the chemical equilibrium, in the limit $\beta A_1 \gg 1$, on neglecling the exponential $e^{-\beta A_1}$ and the small ratio c_1 the reciprocal of the degree of coupling (5.19) takes the extraordinarily simple form:

$$\epsilon^{-1} = \frac{\tau_M(2' \leftrightarrow 2'')}{\tau_M(1' \leftrightarrow 1'')}(1 + c_2 e^{-\beta A_2}). \tag{6.8}$$

In the same approximation the exponential $e^{\beta A_2}$ becomes directly proportional to the flux J_2. On multiplying Eq. (6.8) by this flux we get the relation

$$J_1 \propto 1 + c_2^{-1} \frac{J_2(A_2)}{J_2(0)}, \tag{6.9}$$

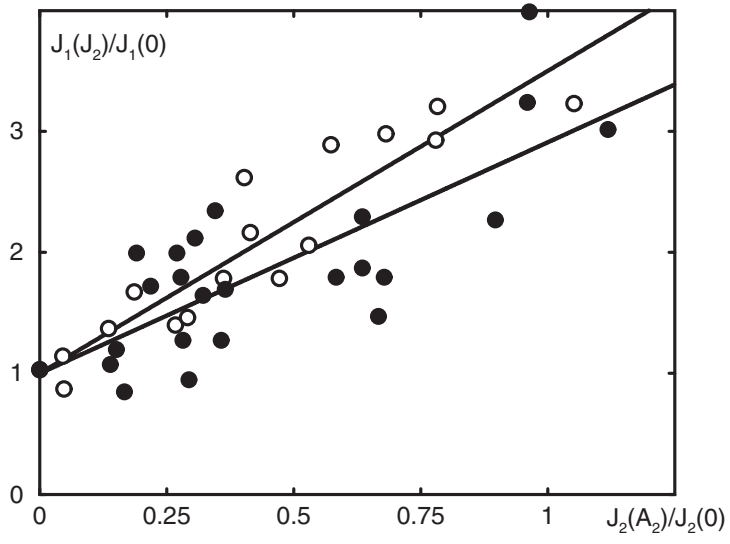

Fig. 15. Fit of Eq. (6.9) to the data of He *et al.*,[62] Fig. 4A. We have assumed that, following Eq. (6.3), the exponential $e^{\beta A_2}$ equals directly to the ratio $J_2(A_2)/J_2(0)$. The black circles correspond to slow fibers and the white circles, to fast 2A fibers in the terminology of ref. 62. The fitted values of the ratio c_2 were found to equal 0.52 and 0.40 for the slow and the fast fibers, respectively.

which states an approximately linear dependence between the rate of ATP utilisation and the rate of the muscle shortening. Figure 15 shows how this dependence fits the data of He *et al.*[62] The ratio c_2, of a value of the order $1/2$, appears to control the *Fenn effect*—a decrease of the rate of ATP consumption with reducing the muscle shortening rate. Contrary to the ratio c_1, the ratio c_2 is not small.

Equation (6.9) gives an idea of the character of the J_1 dependence on the load. To get the full expression for the ATPase activity as a function of the ATP concentration we can use Eq. (6.8) and formulae (5.24) to (5.26) for the parameters τ_{+2}, τ_{-2} and τ_{02}, derived on assuming inequalities (5.16) and putting $e^{-\beta A_1} = 0$. For the condition (6.1) to be satisfied the mean first passage time $\tau_{E_2}(2' \to 2'')$ has to be much longer than $\tau_{E_2}(2'' \to 2')$ and all the remaining transition state theory rate constants. Experimental data (Fig. 11) suggest that, indeed, the times of the very bimolecular steps are negligibly small. As a consequence, we have

$$\tau_{-2} e^{\beta A_2^{st}} = K_+^{-1} [R_1]_0 \, \tau_{02} = \tau_{E_2}(2' \to 2''), \tag{6.10}$$

where

$$K_+ = [R_1]^{eq} [E_1]^{eq} / [E_2]^{eq} \tag{6.11}$$

represents the apparent dissociation constant in the Michaelis–Menten equation (5.27). Simultaneously, the ATPase turnover number

$$k_+ = \frac{e^{\beta A_2} - e^{\beta A_2^{\mathrm{st}}}}{\tau_{\mathrm{E}_2}(2' \to 2'')} \epsilon^{-1}. \tag{6.12}$$

The Michaelis–Menten type dependence of the ATPase activity J_1 on the ATP concentration $[\mathrm{R}_1]$ was observed for the case of the actomyosin motor both in the absence of the load[25] and for nonzero A_2.[64] Also the velocity of actin filament translocation over heavy meromyosin, proportional to J_2, depend on the ATP concentration in the Michaelis–Menten manner.[65] The values of the Michaelis constant K_+ both for J_1 and J_2 are similar, of the order of 10^{-4}M.[25, 64, 65]

For molecular motors the degree of coupling (5.7) has a meaning of number of steps made by the motor per one ATP molecule hydrolysed. The ratio of the working stroke distance to the distance traveled per one hydrolytic cycle is refered to as a *duty ratio* r.[66] Directly from the definition it follows that the duty ratio and the degree of coupling are in the inverse proportionality relation:

$$r \propto \epsilon^{-1}. \tag{6.13}$$

As the exponential $e^{\beta A_2}$ is directly proportional to the flux J_2, Eq. (6.8) represents a hyperbolic dependence of the duty ratio on the sarcomere shortening velocity. This is indeed observed experimentally.[62]

During one ATPase cycle the myosin head transits only once through the state E_1 where the working stroke takes place. For skeletal muscle myosin the working stroke distance equals ~ 5 nm[34, 35, 40] and the duty ratio varies from 0.07 (unloaded sarcomere) to 0.3 or more.[62] In the conventional approach[66] the ratio (6.8) is assumed to equal unity (no slippage) whereas the distance of a single step to a varying multiple of the actin filament period, 36 nm (such a large step is supposed to be possible due to the cooperative organization of the whole assembly of the myosin heads in a sarcomere). However, recent studies clearly demonstrate that a single myosin head moves along the actin filament with much smaller regular steps of ~ 5 nm, which is an actin molecule diameter,[67] and instead, multiple steps can be produced during a single ATPase turnover.[68] There is no reason to doubt that the actin heads behave in a similar manner in the assembly. As a consequence, because the step and the working stroke distances approximately equal each other, the ratio (6.8) should exactly coincide with the duty ratio:

$$\epsilon^{-1} = r. \tag{6.14}$$

In order to fit the experimental data, the ratio $\tau_M(2' \leftrightarrow 2'')/\tau_M(1' \leftrightarrow 1'')$ must be of the order $1/20$. The long mean first-passage time $\tau_M(1' \leftrightarrow 1'')$ can be explained by the necessity of a twofold melting and recrystallization of the SH1-SH2 helix[39, 60, 61] during a transition from the substate $1'$ to $1''$ and back, cf. Fig. 12. The relatively short mean first-passage time $\tau_M(2' \leftrightarrow 2'')$ and the even shorter mean first-passage time $\tau_M(2' \to 2'')$ are the reason why, before coming back to the strongly attached state E_1, the myosin head can stochastically undergo several mechanical cycles through the detached state E_2. The direction of that motion is determined by a large disproportion between the times $\tau_{E_2}(2'' \to 2')$ and $\tau_{E_2}(2' \to 2'')$. It is the latter time that determines the motor velocity, cf. Eq. (6.12).

The scheme given in Fig. 8 represents the mechanochemical cycle of the actomyosin motor seen from the point of view of the myosin molecule. In Fig. 16(a) the very mechanical part of that cycle is presented as seen from the point of view of the entire motor motion, and the numbering of *positions* of the myosin head along the actin track is given (the index l). A transition from the substate $2''_l$ to either the substate $2'_l$ or $2'_{l+1}$ is possible, which corresponds to the motion back and forth the actin filament, respectively. Contrary to Fig. 8, the vertical axes on Fig. 16 represent the free energy levels of individual gates. The external force A_2 exerted by a cargo does not influence the free energy of any conformational substate but induces a difference between the myosin-actin binding free energies before and after the translation. As a consequence, for the negative A_2, the diagram is constantaneously ascending.

The very chemical cycle of the actomyosin motor is shown in Fig. 16(b) where the index n indicates the *reaction progress*—a number of ATP molecules hydrolized. Here a departure from chemical equilibrium results in changes of the free energy levels of the whole macromolecule by A_1 in each cycle.[19] It is the progress of the ATPase cycle that can cause a descend of the free-energy level diagram vs position along the actin track. Figure 16(c) presents the case when both cycles proceed alternatively: translation by a step, reaction, translation by a step, reaction, etc., which corresponds to the value of the degree of coupling $\epsilon = 1$. But ϵ can be both smaller and greater than unity. Such a more general case with possibly repeated both mechanical and chemical cycles needs a three-dimensional presentation.[69] In fact, the degree of coupling ϵ, in the case of the actomyosin motor proved exacly to coincide with the reciprocal duty ratio r, is several times larger than unity.

In the detached state E_2 and in the weakly-attached state M the free energies of the entrance and exit gates do not differ very much. However, in the strongly-attached state E_1 the exit gate has much lower free energy than the entrance gate. That the substate $1'$ has much lower free energy

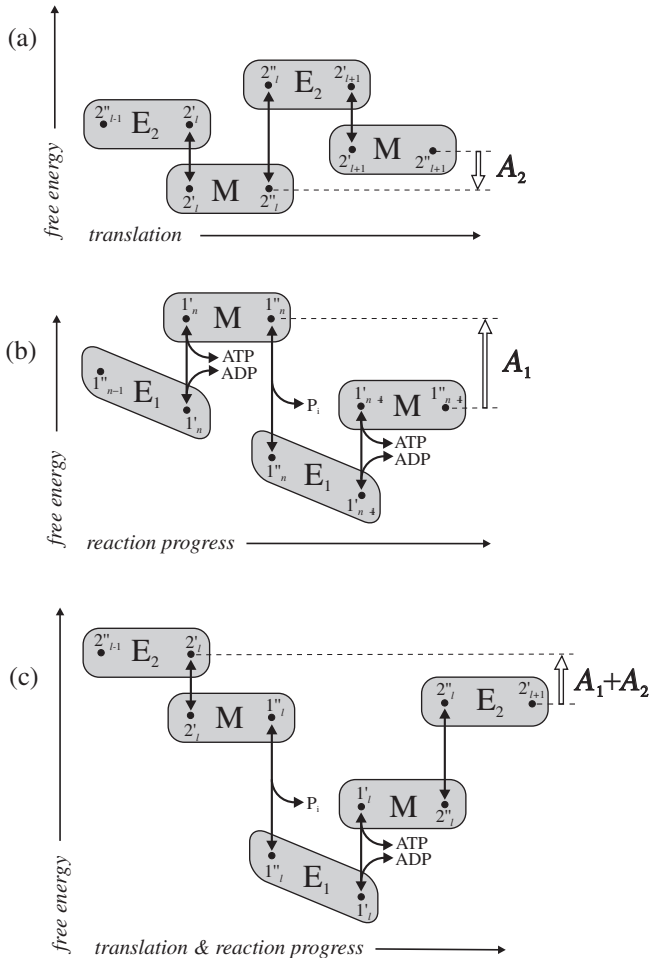

Fig. 16. (a) Mechanical cycle of the actomyosin motor as seen from the point of view of the motor motion. Numbering of positions of the myosin head along the actin track is given. (b) The very chemical cycle; index n indicates the reaction progress—a number of ATP molecules hydrolized. (c) Mechanical cycle alternatig the chemical cycle with the degree of coupling $\epsilon = 1$. The vertical axis represents the free energy of the gates. The chemical force A_1 and the mechanical force A_2 are measures of the departure from equilibrium.

than $1''$ follows, e.g., from its much higher steady-state occupation observed in EPR studies.[42] The drop of the free energy in the transition $1'' \to 1'$ of the myosin head strongly attached to the actin filament corresponds, of course, to the power stroke. However, no details of the power stroke mechanism are important for the action of the actomyosin motor.

Three fundamental parameters of the theory presented are the three first-passage times $\tau_M(1' \leftrightarrow 1'')$, $\tau_M(2' \leftrightarrow 2'')$ and $\tau_{E_2}(2' \to 2'')$ within M and E_2 but not E_1.

7. SUMMARY

Substantial majority of biochemical processes are controlled and gated by purely stochastic dynamics of conformational transitions in the protein enzymes involved. In order to make it possible to calculate the steady-state reaction fluxes in such processes we developed the Hill's technique of summing up the directional diagrams of stochastic dynamics. We applied this technique to a single enzymatic reaction and two coupled enzymatic reactions with several chemical steps gated by conformational transition dynamics of arbitrary type. The case of two coupled reactions was considered as representing the biologically important process of free energy transduction. Serious simplifications of the relevant formulae were obtained after assumption that this process is highly asymmetrical.

Far from equilibrium, when the reaction products are immediately taken from the system, the stady-state reaction fluxes calculated for gated (and only for such) enzymatic reactions appeared to obey the conventional Michaelis–Menten type dependence on the substrate concentration with parameters related to the equilibrium (transition state theory) rate constants and various mean first-passage times. These are to be determined within a definite model of conformational transition dynamics that can be found in detailed research of a definite problem. A consequence of the slow character of intramolecular dynamics is the lack of a direct relationship between the parameters of the steady-state kinetics and the complete (nonequilibrium) rate constants of particular component reactions. The mean first passage times in Eqs. (4.12) to (4.14), (5.19) to (5.21) and (5.24) to (5.26) are between the succeeding gates and not between the "typical" average states and the gates as in the full expression for the rate constant (3.7). We would like to conclude this result with a few, maybe speculative, comments.

The first comment concerns the role of the equilibrium rate constants in enzymatic catalysis. On assuming that the billions years lasting biological evolution acted so as to optimize the rate of enzymatic reaction and that the optimum rate is the fastest possible, one can speculate that the present day enzymes have the entrance and the exit gates for the reaction very close to each other so that the corresponding mean first-passage times are negligible. Puttig them equal to zero in Eqs. (4.12) to (4.14) results in the reconstruction of simple conventional expressions[16] but with

the full reaction rate constants replaced by their transition state theory counterparts. This could explain the applicability of the transition state theory for description of enzymatic catalysis, commonly assumed by most enzymologists.[16]

The second comment concerns the role of the mean first-passage times between the gates in the control of enzymatic catalysis. The activity of protein enzyme can change greatly upon binding an effector molecule. Conventional approach to heterotropic allosteric regulation, in particular noncompetitive inhibition, assumes the effector binding to induce long-rage *structural* changes.[16] However, there is serious evidence that it can induce some *dynamical* changes as well.[70–73] Our theory predicts the enzyme turnover number to depend on both the equilibrium rate constants and the mean first-passage times between the entrance and exit gates. The former are determined by the structure but the latter, by the dynamics. It is physically reasonable to suppose that some inhibitor molecules can act so as to increase the mean first-passage times between the gates rather then to decrease the equilibrium rate constants. The importance of this supposition, if actually true, in particular for pharmacology, can hardly be overestimated.

Contrary to the single enzymatic reactions in which the mean first-passage times between conformational substates of the enzyme seem to be negligible in the optimum conditions, in the case of the free energy transduction processes those times appear to be of the fundamental importance. Our theory of the actomyosin motor is based on three such times: $\tau_M(1' \leftrightarrow 1'')$, $\tau_M(2' \leftrightarrow 2'')$ and $\tau_{E_2}(2' \to 2'')$, cf. Fig. 8 and Eqs. (6.4) to (6.12), and these are, in fact, the only parameters of the theory. The time $\tau_M(1' \leftrightarrow 1'')$ is some 20 times longer than the time $\tau_M(2' \leftrightarrow 2'')$ and this elucidates why the degree of coupling ϵ, following Eq. (6.8), can have a value greater than unity. It agrees very well with the recently demonstrated multiple stepping produced by a single myosin head during just one ATPase cycle.[67, 68]

The scheme in Fig. 8 represents a generalization and, simultaneously, a contraction of the thermal ratchet models extensively discussed in recent years.[51–54] Contrary to the hitherto considered models, the present model is not necessarily one-dimensional—the shaded boxes symbolize arbitrary lattices of conformational substates, in particular they can be fractal lattices.[11] On the other hand, contrary to our model with gated binding-rebinding transitions, the thermal ratchet models were originally considered for delocalized transitions. In such a case the ATP concentration dependence of the output flux displays a maximum (the phenomenon of stochastic resonance). No such maximum is observed experimentally, on the contrary, what is observed is a standard Michaelis–Menten dependence, in

agreement with our prediction, Eq. (5.27). This can be considered as one more argument for the gated mechanism of protein involving reactions assumed in the present paper.

ACKNOWLEDGMENTS

The study has been supported in part by the Polish State Committee for Scientific Research (projects 2 P03B 056 18 and 2 P03B 128 18).

REFERENCES

1. J. A. McCammon and S. C. Harvey, *Dynamics of Proteins and Nucleic Acids* (Cambridge University Press, Cambridge, 1987).
2. C. L. Brooks III, M. Karplus, and B. M. Pettitt, *Proteins: A Theoretical Perspective of Dynamics, Structure and Thermodynamics,* Advances in Chemical Physics, Vol. 71 (Wiley, New York, 1988).
3. H. Frauenfelder, S. G. Sligar, and P. G. Wolynes, The energy landscapes and motions of proteins, *Science* **254**:1598–1603 (1991).
4. H. Frauenfelder, P. G. Wolynes, and R. H. Austin, Biological physics, *Revs. Mod. Phys.* **71**:S419–S430 (1999).
5. M. Kurzyński, A synthetic picture of intramolecular dynamics of proteins. Towards a contemporary statistical theory of biochemical processes, *Prog. Biophys. Molec. Biol.* **69**:23–82 (1998).
6. B. Widom, Molecular transitions and chemical reaction rates, *Science* **148**:1555–1560 (1965).
7. B. Widom, Reaction kinetics in stochastic models, *J. Chem. Phys.* **55**:44–92 (1971).
8. S. G. Northrup and J. T. Hynes, The stable states picture of chemical reactions. I. Formulation for rate constants and initial condition effects, *J. Chem. Phys.* **73**:2700–2714 (1980).
9. M. Kurzyński, Protein machine model of enzymatic reactions gated by enzyme internal dynamics, *Biophys. Chem.* **65**:1–28 (1997).
10. M. Kurzyński, Diffusion on fractal lattices–a statistical model of chemical reactions involving proteins, *Acta Phys. Polon. B* **28**:1853–1889 (1997).
11. M. Kurzyński, K. Palacz, and P. Chełminiak, Time course of reactions controlled and gated by intramolecular dynamics of proteins: Predictions of the model of random walk on fractal lattices, *Proc. Natl. Acad. Sci. USA* **95**:11685–11690 (1998).
12. D. Beece, L. Eisenstein, H. Frauenfelder, D. Good, M. C. Marden, L. Reinisch, A. H. Reynolds, L. B. Sorensen, and K. T. Yue, Solvent viscosity and protein dynamics, *Biochemistry* **19**:5147–5157 (1980).
13. N. G. van Kampen, *Stochastic Processes in Physics and Chemistry* (North-Holland, Amsterdam, 1981).
14. M. Kurzyński, Internal dynamics of biomolecules and statistical theory of biochemical processes, *Phys. A* **285**:29–47 (2000).
15. L. A. Blumenfeld, *Problems of Biological Physics*, Springer Series in Synergetics, Vol. 7 (Berlin, 1981).
16. A. Fersht, *Enzyme Structure and Mechanism*, 2nd Ed. (Freeman, New York, 1985).
17. P. Chełminiak and M. Kurzyński, Mean first-passage time in the steady-state kinetics of biochemical processes, *J. Molec. Liquids* **86**:319–325 (2000).

18. R. J. Wilson, *Introduction to Graph Theory*, 4th Ed. (Adison Wesley Longman, London, 1996).
19. T. L. Hill, *Free Energy Transduction and Biochemical Cycle Kinetics* (Springer, New York, 1989).
20. M. Kurzyński, Enzymatic catalysis as a process controlled by protein conformational relaxation, *FEBS Lett*. **328**:221–224 (1993).
21. L. Stryer, *Biochemistry*, 4th Ed., Chaps. 12 and 15 (Freeman, New York, 1995).
22. H. V. Westerhoff and K. van Dam, *Thermodynamics and Control of Biological Free-Energy Transduction* (Elsevier, Amsterdam, 1987).
23. R. W. Lymn and E. W. Taylor, Mechanism of adenosine triphosphate hydrolysis by actomyosin, *Biochemistry* **10**:4617–4624 (1971).
24. E. Eisenberg and T. L. Hill, Muscle contraction and free energy transduction in biological systems, *Science* **227**:999–1006 (1985).
25. Y.-Z. Ma and E. W. Taylor, Kinetic mechanism of myofibril ATPase, *Biophys. J.* **66**:1542–1553 (1994).
26. Y. Zhao and M. Kawai, Kinetic and thermodynamic studies of the cross-bridge cycle in rabbit psoas muscle fibers, *Biophys. J.* **67**:1655–1668 (1994).
27. J. Howard, *Mechanics of Motor Proteins and the Cytoskeleton* (Sinauer Associates, Sunderland, 2001).
28. C. S. Peskin and G. Oster, Coordinated hydrolysis explains the mechanical behaviour of kinesin, *Biophys. J.* **68**:202s–211s (1995).
29. T. Duke and S. Leibler, Motor protein mechanics: A stochastic model with minimal mechanochemical coupling, *Biophys. J.* **71**:1235–1247 (1996).
30. H. Wang and G. Oster, Energy transduction in the F_1 motor of ATP synthase, *Nature* **396**:279–282 (1998).
31. H. Wang, T. Elston, A. Mogilner, and G. Oster, Force generation in RNA polymerase, *Biophys. J* **74**:1186–1202 (1998).
32. F. Jülicher and R. Bruinsma, Motion of RNA polymerase along DNA: A stochastic model, *Biophys. J.* **74**:1169–1185 (1998).
33. H. E. Huxley, The mechanism of muscular contraction, *Science* **164**:1356–1366 (1969).
34. J. T. Finer, R. M. Simmons, and J. A. Spudich, Single myosin molecule mechanics: piconewton forces and nanometer steps, *Nature* **368**:113–119 (1994).
35. T. Q. P. Uyeda, P. D. Abramson, and J. A. Spudich, The neck region of the myosin motor domain acts as a lever arm to generate movement, *Proc. Natl. Acad. Sci. USA* **93**:4459–4464 (1996).
36. I. Rayment, H. M. Holden, M. Whittaker, C. B. Yohn, M. Lorenz, K. C. Holmes, and R. A. Miligan, Structure of the actin-myosin complex and its implications for muscle contraction, *Science* **261**:58–65 (1993).
37. A. J. Fisher, C. A. Smith, J. B. Thoden, R. Smith, K. Sutoh, H. M. Holden, and I. Rayment, X-ray structure of the myosin motor domain of *Distyostelium discoideum* complexed with $MgADP \cdot BeF_x$ and $MgADP \cdot AlF_4^-$, *Biochemistry* **34**:8960–8972 (1995).
38. R. Dominiquez, Y. Freyzon, K. M. Trybus, and C. Cohen, Crystal structure of a vertebrate smooth muscle myosin motor domain and its complex with the essential light chain: Visualization of the pre-powerstroke state, *Cell* **94**:559–571 (1998).
39. A. Houdusse, A. G. Szent-Györgi, and C. Cohen, Three conformational states of scallop myosin S1, *Proc. Natl. Acad. Sci. USA* **97**:11238–11243 (2000).
40. M. Whittaker, E. M. Wilson-Kubalek, J. E. Smith, L. Faust, R. A. Milligan, and H. L. Sweeney, A 34-A movement of smooth muscle myosin on ADP release, *Nature* **378**:748–751 (1995).
41. M. Walker, X-Z. Zhang, W. Jiang, J. Trinick, and H. D. White, Observation of transient disorder during myosin subfragment-1 binding to actin by stopped-flow fluorescence and

milisecond time resolution cryomicroscopy: Evidence that the start of the crossbridge power stroke in muscle has variable geometry, *Proc. Natl. Acad. Sci. USA* **96**:465–470 (1999).
42. J. E. Baker, I. Brust-Mascher, S. Ramachandran, L. E. W. LaConte, and D. D. Thomas, A large and distinct rotation of the myosin light chain domain occurs upon muscle contraction, *Proc. Natl. Acad. Sci. USA* **95**:2944–2949 (1998).
43. J. E. Baker, L. E. W. LaConte, I. Brust-Mascher, and D. D. Thomas, Mechanochemical coupling in spin-labeled, active, isometric muscle, *Biophys. J.* **77**:2657–2664 (1999).
44. D. M. Warshaw, E. Hayes, D. Gaffney, A-M. Lauzon, J. Wu, G. Kennedy, K. Trybus, S. Lowey, and C. Berger, Myosin conformational states determined by single fluorophore polarization, *Proc. Natl. Acad. Sci. USA* **95**:8034–8039 (1998).
45. J. E. T. Corrie, B. D. Brandmeyer, R. E. Ferguson, D. R. Trentham, J. Kendrick-Jones, S. C. Hopkins, U. A. van der Heide, Y. E. Goldman, C. Sabido-David, R. E. Dale, S. Criddle, and M. Irving, Dynamic measurement of myosin light-chain-domain tilt and twist in muscle contraction, *Nature* **400**:425–430 (1999).
46. Y. Suzuki, T. Yasunaga, R. Ohkura, T. Wakabayashi, and K. Sutoh, Swing of the lever arm of a myosin motor at the isomerization and phosphate-release step, *Nature* **396**:380–383 (1998).
47. M. Xiao, H. Li, G. E. Snyder, R. Cooke, R. G. Yount, and P. R. Selvin, Conformational changes between the active-site and regulatory light chain of myosin as determined by luminescence resonance energy transfer: The effect of nucleotides and actin, *Proc. Natl. Acad. Sci. USA* **95**:15309–15314 (1998).
48. J. Xu and D. D. Root, Conformational selection during weak binding at the actin and myosin interference, *Biophys. J.* **79**:1498–1510 (2000).
49. T. A. J. Duke, Molecular model of muscle contraction, *Proc. Nat. Acad. Sci. USA* **96**:2770–2775 (1999).
50. R. M. Krupka, Force generation, work, and coupling in molecular motors, *Biophys. J.* **70**:1863–1871 (1996).
51. N. J. Cordova, B. Ermentrout, and G. F. Oster, Dynamics of sigle-motor molecules: The thermal ratchet model, *Proc. Nat. Acad. Sci. USA* **89**:339–343 (1992).
52. R. D. Astumian and M. Bier, Mechanochemical coupling of the motion of molecular motors to ATP hydrolysis, *Biophys. J.* **70**:637–653 (1996).
53. A. Parmeggiani, F. Jülicher, A. Ajdari, and J. Prost, Energy transduction in isothermal ratchets: Generic aspects and specific examples close to and far from equilibrium, *Phys. Rev. E* **60**:2127–2140 (1999).
54. M. E. Fischer and A. B. Kolomeisky, The force exerted by a molecular motor, *Proc. Natl. Acad. Sci. USA* **96**:6597–6602 (1999).
55. J. E. Baker and D. D. Thomas, Thermodynamics and kinetics of a molecular motors ensemble, *Biophys. J.* **79**:1731–1736 (2000).
56. E. M. Ostap, V. A. Barnett, and D. D. Thomas, Resolution of three structural states of spin-labeled myosin in contracting muscle, *Biophys. J.* **69**:177–188 (1995).
57. Ch. J. Berger and D. D. Thomas, Rotational dynamics of actin-bound intermediates of the myosin adenosine triphosphate cycle in myofibrils, *Biophys. J.* **67**:250–261 (1994).
58. N. Volkmann and D. Hanein, Actomyosin: law and order in motility, *Curr. Opin. Cell Biol.* **12**:26–34 (2000).
59. B. Adhikari, K. Hideg, and P. G. Fajer, Independent mobility of catalytic and regulatory domains of myosin heads, *Proc. Natl. Acad. Sci. USA* **94**:9643–9647 (1997).
60. K. Konno, K. Ue, M. Khoroshev, H. Martinez, B. Ray, and M. F. Morales, Consequences of placing an intramolecular crosslink in myosin S1, *Proc. Natl. Acad. Sci. USA* **97**:1461–1466 (2000).

61. L. K. Nitao and E. Reisler, Actin and temperature effects on the cross-linking of the SH1-SH2 helix in myosin subfragment 1, *Biophys. J.* **78**:3072–3080 (2000).
62. Z-H. He, R. Bottinelli, M. A. Pellegrino, M. A. Ferenczi, and C. Reggiani, ATP consumption and efficiency of human single muscle fibers with different myosin isoform composition, *Biophys. J.* **79**:945–961 (2000).
63. E. Pate, K. Franks-Skiba, and R. Cooke, Depletion of phosphate in active muscle fibers probes actomyosin states with the powerstroke, *Biophys. J.* **74**:369–380 (1998).
64. C. Lionne, F. Travers, and T. Barman, Mechanochemical coupling in muscle: Attempts to measure simultaneously shortening and ATPase rates in myofibrils, *Biophys. J.* **70**:887–895 (1996).
65. I. Amitani, T. Sakamoto, and T. Ando, Link between the enzymatic kinetics and mechanical behaviour in an actomyosin motor, *Biophys. J.* **80**:379–397 (2001).
66. J. Howard, Molecular motors: structural adaptations to cellular functions, *Nature* **389**:561–567 (1997).
67. K. Kitamura, M. Tokunaga, A. H. Iwane, and T. Yanagida, A single myosin head moves along an actin filament with regular steps of 5.3 nanometers, *Nature* **397**:129–134 (1999).
68. A. Ishijima, H. Kojima, T. Funatsu, M. Tokunaga, H. Higuchi, H. Tanaka, and T. Yanagida, Simultaneous observation of individual ATPases and mechanical events by a single myosin molecule during interaction with actin, *Cell* **92**:161–171 (1998).
69. D. Keller and C. Bustamante, The mechanochemistry of molecular motors, *Biophys. J.* **78**:541–556 (2000).
70. O. Jardetzky, Protein dynamics and conformational transitions in allosteric proteins, *Prog. Biophys. Molec. Biol.* **65**:171–219 (1996).
71. J. T. Stivers, C. Abeygunawardana, A. S. Mildvan, and C. P. Whitman, ^{15}N NMR relaxation studies of free and inhibitor-bound 4-oxalocrotonate tautomerase: Backbone dynamics and entropy changes of an enzyme upon inhibitor binding, *Biochemistry* **35**:16036–16047 (1996).
72. M. E. Hodsdon and D. P. Cistola, Ligand binding alters the backbone mobility of intestinal fatty acid-binding protein as monitored by ^{15}N NMR relaxation and ^{1}H exchange, *Biochemistry* **36**:2278–2290 (1997).
73. A. N. Hoofnagle, K. A. Resing, E. J. Goldsmith, and N. G. Ahn, Changes in protein conformational mobility upon activation of extracellular regulated protein kinase-2 as detected by hydrogen exchange, *Proc. Natl. Acad. Sci. USA* **98**:956–961 (2001).